ADAPTIVE TRANSMISSION TECHNIQUES IN WIRELESS FADING CHANNELS

CHEN XUN

NATIONAL UNIVERSITY OF SINGAPORE

2005

ADAPTIVE TRANSMISSION TECHNIQUES IN WIRELESS FADING CHANNELS

CHEN XUN

A THESIS SUBMITTED

FOR THE DEGREE OF MASTER OF ENGINEERING

DEPARTMENT OF ELECTRICAL & COMPUTER ENGINEERING

NATIONAL UNIVERSITY OF SINGAPORE

2005

Acknowledgments

This work has been supported by many people to whom I wish to express my gratitude. I wish to thank my advisors, Dr. Chai Chin Choy and Dr. Chew Yong Huat, who are from Institute for Infocomm Research. Their attitude and encouragement have provided inspiration to many of my ideas and undoubtedly have given dynamism to my research studies. I want to thank them for giving opportunities in blossoming my research idea. Under their guidance I went on a path that I am confident I will provide numerous research topics for the years to come. During the past two years in which we worked closely together they have helped me in learning the way to be an independent researcher. I hope they are proud of me as I am proud to have them as my supervisors.

Special thanks go to my colleagues who are working in the ECE-I^{2}R Wireless Communications Laboratory and Institution for Infocomm Research (I^{2}R): Dr. Ronghong Mo, Mr. Xiaoyu Hu, Mr. Jianxin Yao and Ms. Kainan Zhou. I really appreciate those valuable discussions with them. Furthermore, I would thank I^{2}R for providing the scholarship in the past two years.

Finally, I shall thank my parents and elder sister for their never-ending support.

Summary

Fading and interference are the two main factors that degrade the performance of wireless communication systems. To improve the performance of current and next generation wireless systems, advanced techniques are needed to alleviate the deleterious impacts of fading and interference. Among them, adaptive transmission techniques are of significance.

In this thesis, the application of two adaptive transmission techniques: transmitter power adaptation and adaptive modulation, are considered and studied.

Firstly, we develop a power control scheme for the interference-limited Nakagami fading channels to minimize the outage probabilities of users. The upper and lower bounds that we have derived for the outage probability help us to solve the minimization problem in a simpler way by using a modified SIR-balancing model.

Secondly, we examine the performance of adaptive **M**-ary Quadrature Amplitude Modulation (MQAM) system in the presence of Nakagami fading, log-normal shadowing and co-channel interference. We derive an approximate expression of the *probability density function* (PDF) for the received *signal-to-interference ratio* (SIR). Through the numerical results obtained, we present the impacts of fading and shadowing on the performance of adaptive modulation in the above system.

Finally, attention is drawn on the problem of transmitter power allocation in multiple-input multiple-output (MIMO) system. A novel sub-optimal power

allocation algorithm is derived based on the computation-complex optimal algorithm. The proposed algorithm is simpler in computation, while it presents a satisfying performance in terms of the achievable data throughput and the power efficiency.

Table of Contents

List of Tables

List of Figures

List of Notations

N	the number of active users(transmitter-receiver pairs) in the system
G_{ij}	the path gain from transmitter j to receiver i
P_i	the transmitted power from transmitter i
T	the total throughput of the system
p_i	the allocated power in the ith eigenchannel
P_T	the total available transmitter power for power allocation
λ_i	the channel gain in the ith eigenchannel
σ_N^2	the Gaussian noise power
l	the number of eigenchannels with non-zero channel gain
α_{ij}	the fading gain in the channel from transmitter j to receiver i
N_T	the number of antennas at the transmitter
N_R	the number of antennas at the receiver
$\mathbf{H}$	the $N_R \times N_T$ channel gain matrix
h_{ij}	the channel gain from transmit antenna j to receive antenna i
β	the pass loss exponent
ξ	the shadowing factor (dB spread)
r_{ij}	the amplitude of the received signal from transmitter j to receiver i
Ω_{ij}	the average received signal power from transmitter j to receiver i
K	the Ricean Factor
m_{ij}	the fading index of Nakagami fading channel from transmitter j to receiver i

ς	the given protection ratio or threshold of SIR specified by QoS requirement
M_i	the equivalent fading index of the Nakagami fading interference experienced by receiver i
SIRM_i	the signal-to-interference margin of the received signal at receiver i
$P_{L,i}^{out}$	the lower bound of the outage probability of the received signal at receiver i
$P_{U,i}^{out}$	the upper bound of the outage probability of the received signal at receiver i
F_{ij}	the path loss gain of the link from B_j to U_i
B_i	base station i
U_i	user i
γ_i	the received SIR at user/receiver i
$\overline{\gamma}_i$	the average received SIR at user/receiver i
s	the number of constellation sizes
S_i	the constellation size of MQAM, $S_i = 2^i$ with $0 \leq j \leq s$
Υ	the target BER
$T_u^{(i)}$	the throughput of user i
T_{av}	the average throughput per user
P_{av}^{out}	the average outage probability per user
τ_i	the BER in the ith eighenchannel
κ_i	the ith SIR threshold in the adaptive modulation system, $0 \leq i \leq s$
$T_c^{(i)}$	the throughput in the ith eigenchannel
$\text{PITIR}_k^{i \to j}$	the PITIR of the action which is to change the constellation size from S_j to S_i in the kth eigenchannel

LMD_i	the ith LMD, or equivalently, the LMD in the ith position (refer to Fig. 5.1)
$b_{to,i}$	the total throughput in the power allocation specified by LMD_i
N_b	the number of different LMD
$p_{to,i}$	the total allocated power in the power allocation specified by LMD_i
$t_{i,j}$	the throughput in the jth eigenchannel in the power allocation specified by LMD_i
$\Gamma(a)$	the Gamma function
$\Gamma(a,b)$	the incomplete Gamma function

List of Abbreviations

AQAM	Adaptive Quadrature Amplitude Modulation
AWGN	Additive White Gaussian Noise
CDF	Cumulative Density Function
CDMA	Code Division Multiple Access
CEM	Certainty-Equivalent Margin
CSI	Channel State Information
DPC	Distributed Power Control
DCPC	Distributed Constrained Power control
DMT	Discrete Multi-Tone
FDMA	Frequency Division Multiple Access
GSM	Global System of Mobile Communications
LoS	Line of Sight
LRP	Long-Range Prediction
MIMO	Multiple-Input Multiple-Output
MISO	Multiple-Input Single-Output
MMSE	Minimum Mean-Square Error
MQAM	$\boldsymbol{M}$-ary Quadrature Amplitude Modulation
PDF	Probability Density Function
OFDM	Orthogonal Frequency Divided Multiplexing
PSAM	Pilot Symbol-Assisted Modulation
QAM	Quadrature Amplitude Modulation

QoS	Quality of Service
BER	Bit Error Rate
SINR	Signal-to-Interference-plus-Noise Ratio
SIR	Signal-to-Interference Ratio
SIMO	Single-Input Multiple-Output
SISO	Single-Input Mingle-Output
SNR	Signal-to-Noise Ratio
TDMA	Time Division Multiple Access

Chapter 1

Introduction

1.1 Adaptive Transmission Techniques

To maintain requirements on the *quality of service* (QoS) for users, it is important to efficiently combat both fading and interference in wireless communication systems. However, it becomes difficult when a large number of users are active in the system because each user's service quality is closely related to how other users are served. In this work, we focus on two techniques that have been developed to solve the problem: *transmitter power adaptation* and *adaptive modulation*.

1.1.1 Transmitter Power Adaptation

In this work, we study transmitter power control in cellular system and transmitter power allocation in MIMO system. In transmitter power control, we adjust the transmitter power according to the link quality; in transmitter power allocation, we distribute the total transmitter power adaptively among

multiple antennas according to the varying channel states.

1.1.1.1 Transmitter Power Control

Transmitter power control is highly related to the network capacity, especially in the systems where the interference has a significant impact. For example, delay sensitive users with stringent *bit error rate* (BER) requirement can be accommodated by adapting their transmit powers to the channel so as to increase their *signal-to-interference-plus-noise ratio* (SINR) or SIR. However, this might cause an increase in the interference experienced by other users, in turn increasing their BER. On the other hand, as we know, users close to the base station experience a small path loss. If without power control, signals transmitted from users far away from the base station will be buried by the signals transmitted from users that are much closer, which is indeed the famous *near-far* problem in *code division multiple access* (CDMA) system in which the interference is severe.

Thus, to support as many users as possible with QoS requirements, the proper control of the transmitter powers is important. In traditional fix-rate system, QoS requirement is often closely related to the BER which mainly depends on the received SIR. Therefore, the classical power control in fixed-rate system usually aims to find the minimum power assignment that supports the required SIR for as many users as possible.

A simplified mathematical model for the power control problem in an interference-limited system with N active users (or transmitter-receiver pairs) is given below. Denote the transmitted power from transmitter i and the path gain from transmitter j to receiver i by P_i and G_{ij}, respectively. Then the average received SIR at the receiver i, $\overline{\text{SIR}}_i$, is given by

$$\overline{\text{SIR}}_i = \frac{G_{ii}P_i}{\sum\limits_{j\neq i} G_{ij}P_j}\,, \tag{1.1}$$

where $P_i \geq 0$ for $i = 1, 2, \cdots, N$. Consequently, the classical power control problem can be expressed as

$$\overline{\text{SIR}}_i \geq \text{SIR}_{i,req}\,, \qquad \text{for} \quad i = 1, 2, \cdots, N$$

where $\text{SIR}_{i,req}$ is the SIR requirement for receiver i.

The above is also known as SIR-based power control problem, which is possible when the relationship between QoS requirement and the SIR quality is explicit. Many centralized [1–8] and distributed algorithms [9–15] have been developed to solve this problem.

1.1.1.2 Transmitter Power Allocation

The MIMO technique has the great potential to increase the capacity of wireless communication systems. Optimal power allocation can further improve the advantage of MIMO system, especially when the *channel states information*

(CSI) is known to the transmitter. Meanwhile, as power is considered a critical resource in the system, optimizing the power allocation in multiple transmit antennas is essential.

The objective of power allocation is to maximize the total data throughput T of the MIMO system under the total transmit power constraint P_T. By using *singular value decomposition* (SVD), the channel matrix is diagonalized and the set of constituent eigenchannels are obtained. Denote the number of eigenchannels with nonzero channel gain by l. The power allocation problem can then be expressed mathematically as

$$\begin{aligned} \max \quad & T \\ \text{s.t.} \quad & \textstyle\sum_{i=1}^{l} p_i \leq P_T \\ & p_i \geq 0 \quad for \;\; i = 1, \cdots, l \end{aligned} \tag{1.2}$$

where p_i is the allocated power in the ith eigenchannel.

When both transmitter and receiver have access to CSI, the transmitter can adapt the power allocation according to the quality of channel. The optimal power allocation strategy is the well-known waterfilling solution and is given by

$$p_i = \left(\varepsilon - \frac{\sigma_N^2}{\lambda_i^2} \right)^+ \tag{1.3}$$

where ε satisfies

$$\sum_i \left(\varepsilon - \frac{\sigma_N^2}{\lambda_i^2} \right)^+ = P_T \,. \tag{1.4}$$

λ_i is the channel gain of the ith eigenchannel. A suboptimal solution could be allocating equal power across the eigenchannels, that is

$$p_i = \frac{P_T}{l}\,. \tag{1.5}$$

Note that (1.5) is also the traditional power allocation solution when the channel gain matrix is unknown at the transmitter.

1.1.2 Adaptive Modulation

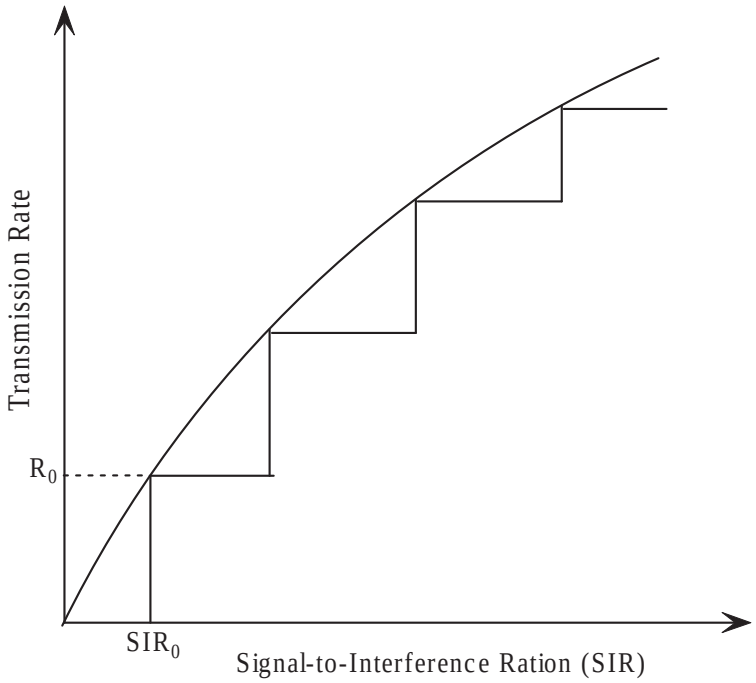

Figure 1.1: An illustration of the relation between transmission rate and SIR.

Adaptive modulation is an important transmission technique employed in variable-rate communication systems, which is achieved through adapting the

modulation rate to the quality of channel which is often in terms of the received SIR. Similar to the traditional fix-rate system, a target BER reflecting the QoS requirements is still specified, however, as the transmission rate is flexible, the required SIR is not fixed. Generally, higher SIR is necessary to support a higher transmission rate while maintaining a specific BER within the same bandwidth. A typical relationship between transmission rate and SIR is presented as an example in Fig. 1.1. When transmission rate is able to be realized at continuous values, the relation is represented by a continuous curve, while in real systems, transmission rate can be only some finite discrete values, therefore the relation is represented by a stepwise line.

During transmission, CSI are to be estimated at the receiver, which is then fed back to the transmitter within a negligible short time. Transmitter determines the transmission rate according to the received SIR and the target BER.

In Fig. 1.1, when the received SIR is below the pre-determined SIR threshold SIR_0, the transmission rate is zero in the case of discrete transmission rate. That is, the transmission is ceased when the channel quality is severely bad. The status that $\mathrm{SIR} < \mathrm{SIR}_0$ is called *outage*. The corresponding transmission rate, R_0 is called *outage rate*.

Since adaptive modulation can efficiently make use of the given bandwidth and thereby achieve higher data rate, it has attracted much attention, and has been adopted in some high speed transmission systems.

1.2 Previous Works

The work in this thesis has covered areas of power adaptation and adaptive modulation. Therefore, we divide the literature survey into two parts.

1.2.1 Transmitter Power Adaptation

1.2.1.1 Transmitter Power Control

As a major technique to combat co-channel interference, power control has been studied extensively. In [1], the power control problem was formulated as a linear programming problem by Bock and Ebstein. Aein [2] showed that the SIR-balancing in noiseless system, i.e., to obtain the same quality on all links, could be reduced to an eigenvalue problem for nonnegative matrices. Such a concept was extended to spread spectrum systems without background noise by Nettleton and Alavi [3] [4]. In [5], Zander derived the optimal power solution for minimizing the outage probability, which was shown to find the maximum achievable SIR that could be achieved simultaneously in all links. Later, Grandhi *et al.* proved the uniqueness of the common balanced SIR and the uniqueness of the positive power solution vector [6]. In [7], the work was extended to the case with nonzero background noise. It was shown that, if there was no constraints on the maximum transmitter power, the SIR could be achieved arbitrarily close to that in the case when the background noise was neglected. The case with maximum transmitter power constraints was investigated by Grandhi *et al.* [13], where the author showed that there would always

be at least one user utilizing the maximum transmitter power.

It should be noted that in most of references mentioned above, the power control algorithms are centralized, i.e., to compute the transmitter power for one link, the information for all other links has to be available. From a practical point of view, as the number of links increases with the number of users in the system, the centralized approach involves added infrastructure, latency and network vulnerability. Therefore, more appealing and simple distributed algorithms have been developed. In Zander's companion paper [9], the distributed balancing algorithm was introduced, which required only the local measurements and was shown to converge to the power solution that achieved the common maximal SIR. In [10], the *distributed power control* (DPC) algorithm was developed and had presented a faster convergency. A more general and realistic algorithm was considered by Foschini and Miljanic [11], in which the receiver noise and a respective target SIR were taken into account. This algorithm could converge to a fixed point of a feasible system either synchronously [11] or asynchronously [12]. In [13], Grandhi *et al.* presented a *distributed constrained power control* (DCPC) algorithm including the background noise and maximum transmitter power constraints. In [14], Jäntti and Kim proposed a second-order iterative power control algorithm to accelerate the rate of convergence compared to the first-order DCPC algorithm. The authors also suggested a block-distributed power control algorithm by applying iterative methods from numerical linear algebra in [15].

When the system becomes congested, the power control solutions may become infeasible. Almgren *et al.* [16] and Yates *et al.* [17] proposed algorithms that reduced the target SIR linearly in order to reduce the probability of an infeasible power control problem. Another way is to remove users from current system. The stepwise removal algorithm [5] and the stepwise maximum interference removal algorithm [18] were proposed. Andersin *et al.* presented the gradual removal restricted algorithm [19] which allowed the removing connections during power updates, and the combined removal/power control algorithm could be performed in a fully distributed way.

1.2.1.2 Transmitter Power Allocation

Transmitter power allocation in MIMO system depends on the availability of CSI.

When the CSI is available at the transmitter, the optimal power allocation that achieves the maximum capacity is well known [20], [21]. In such a case, capacity is achieved by optimally allocating the available total power across the eigenchannels in a "water-filling" fashion [21–24]. To be more specific, the eigenchannels with better quality will be allocated more transmit power to obtain a higher capacity. Ever since then, many optimal power allocation strategies have been developed based on the idea of waterfilling. In [25], a stochastic waterfilling solution was proposed. In [26], the author considered the generalized waterfilling for multiple antenna systems. A closed form expression for the

power allocation for a MISO channel was provided. Jindal *et al.* considered the problem of maximizing sum rate on a multi-antenna downlink [27]. By using a duality, a simple and fast iterative algorithm for optimal power allocation was proposed. For the same problem in [27], it was shown in [28] that in contrast to the conventional waterfilling, the number of users that were allocated power to maximize the sum rate could be a non-monotonic function of the total power for some channel realizations. The optimal power allocation by using waterfilling jointly in the frequency domain and spatial domain was analyzed in [29].

When CSI is not available at the transmitter, but the channel statistics are *a priori* known, an optimal fixed power allocation can be adopted. Foschini and Gans showed that when there was no CSI at the transmitter, the capacity of a MIMO channel was achieved by performing a uniform power allocation [30]. Later, the optimality of the uniform power allocation in terms of ergodic capacity was proved in [21]. The result was extended to the multiuser case in [31]. In addition, the uniform power allocation has been found optimal in non-coherent multiple-antenna channels in the high *signal-to-noise ratio* SNR regime [32].

There are also some works that have studied the optimal power allocation when the CSI is partially available at the transmitter. Visotsky and Madhow considered the second order statistics of channel as partial CSI at the transmitter for *multiple-input single-output* (MISO) system [33]. In [34], Visotsky's results were extended to MIMO channels. In [35], the received SNR is considered as

partial CSI for MISO channels. Roh *et al.* studied the cases where the CSI was partially known to the transmitter in a way that enabled a reduction in the amount of the feedback information. The authors proposed a beamforming method for the power allocation problem.

However, most of the above works assumed continuous modulation order and infinite-length codebook. In [36], the authors considered the power allocation in MIMO system with discrete modulation order and the BER constraint. A QoS based waterfilling algorithm was then proposed. It should be noted that such a problem has been also considered in multicarrier system. Therefore, many previous algorithms [37–41] that have been developed for multicarrier system can be applicable in the case of MIMO system. In [37], an optimal bit allocation algorithm was proposed by adding one bit a time to the channel requiring the smallest additional power to increase its rate. The authors in [38] and [39] developed the sub-optimal algorithm that relied on rounding to achieve the optimal power and bit allocation in *discrete multi-tone* (DMT) system. Krongold *et al.* [40] proposed a computationally efficient algorithm for power and bit allocation by using efficient lookup table searches and a Lagrange- multiplier bisection search. In [41], the author refined the waterfilling process and developed a simplified sub-optimal algorithm for power allocation in multicarrier system.

1.2.2 Adaptive Modulation

Adaptive Modulation has been shown to be a promising technique to improve the transmission performance in radio channels which suffer from shadowing and fading. Bello and Cowan [42] analyzed the performance of on/off transmission, which could be considered as a special case of a two-rate transmission system. In [43], Cavers considered Rayleigh fading channels and suggested a variable-rate transmission scheme in which the data rate was adjusted optimally according to the perceived channel quality. Webb and Steele proposed the *adaptive quadrature amplitude modulation* (AQAM) which employed various star *quadrature amplitude modulation* (QAM) constellations [44] [45]. The work by Webb and Steele stimulated further research in this area. With the advent of *pilot symbol-assisted modulation* (PSAM) [46–48], Otsuke *et al.* employed maximum-minimum distance-based square constellations rather than star constellations in the context of AQAM. In [49], it was shown that the AQAM had promising advantages in terms of spectra efficiency, BER performance and robustness against channel delay spread, when compared to fixed modulation. Various systems employing AQAM were also characterized in [50].

The performance of AQAM scheme was predetermined by the switching levels employed, an initial attempt to find optimum switching levels was made by Webb and Steele [44]. In [44], the SNR values to maintain the specific BER requirement for each modulation mode was obtained by using the BER

curves. These switching levels could ensure the instantaneous BER always below the certain threshold, and were widely used in [51] and [52]. Finding the optimum switching levels that satisfy the target average BER rather than instantaneous BER was studied by Hanzo *et al.* [53–55]. In [53], the authors proposed the employment of a heuristic cost function and applied Powell's optimization method [56]. The scheme in [55] was further improved by employing a modified cost function to guarantee a constant target average BER over the whole operating SNR range [54]. In [55], Lagrangian optimization techniques was applied for deriving globally optimized switching levels. Meanwhile, Paris *et al.* [57] proposed a set of optimal switching thresholds based on a multidimensional optimization technique, in which transmitter power varied according to modulation modes. Chung and Goldsmith [58] derived formulas for determining the optimal switching levels for various AQAM schemes.

In the literature, research efforts have shown the attractive performance of adaptive modulation. In [52], it was demonstrated that using adaptive modulation can provide a 5-10 dB gain over a fixed rate system having only power control in a single user case. In [49], the authors proposed an adaptive modulation system for personal multimedia communications, and they showed that this system could achieve spectrum efficiencies that were three times higher than a traditional system without adaptive modulation. In [52], the adaptive variable-rate variable-power scheme was 17 dB more power efficient than nonadaptive modulation in fading. Qiu and Chawla [59] investigated joint optimization of

modulation and powers to maximize the log-sum of the users' SIR. The authors showed that using adaptive modulation provides a significant throughput advantage even without power control, and they presented that combination of adaptive modulation and suitable power control leads to a significant higher throughput as compared to no power control or using SINR-balancing power control.

As accurate channel state information is of importance to the performance of adaptive modulation, recently, reliable prediction of channel state attracts extensive interest. The capacity of Nakagami multipath fading channels with an average power constraint was studied in [60], and the authors investigated the impact of time delay on the adaptive modulation performance. A. Duel-Hallen *et al.* proposed a novel adaptive *long-range prediction* (LRP) method in [61] [62], which employed an autoregressive model to characterize the fading channel and predicts the future channel state based on past observations by *minimum mean-square error* (MMSE) estimation. The method was further extended in [63]. In [64], the authors proposed an adaptive modulation scheme which used an unbiased quadratic regression of past noisy channel estimates to predict the signal power at the receiver.

1.3 Contributions

The main contributions of this thesis have been published [65–67]. Here a summary on the contributions of the thesis is presented.

Chapter 3

In this chapter, we study the problem of minimizing outage probabilities for interference-limited Nakagami channels. Based on the new upper and lower bounds of the outage probability we have derived, we develop a new performance index that provides us a more general interpretation on power control problem in Nakagami fading channels. Our analysis also helps us view previous results in [68] and [5] in a more general perspective. A new power control algorithm is proposed, which updates the transmitted powers of system users based on the relatively much longer time scale of shadowing, instead of the smaller time scale of fading that is assumed in most of previous work mentioned in Section 1.2.1.1. Our results show that the proposed algorithm includes the similar issue in Rayleigh channel [68] as a special case.

The results have been published in *Proc. VTC'2003 Fall* [65].

Chapter 4

In this chapter, we evaluate the performance of adaptive MQAM system in interference-limited Nakagami fading channels with log-normal shadowing. We use a new approach to derive the approximate expression for the PDF of the instantaneous received SIR by applying previous results in [69] and [70]. Based on the PDF expression of the SIR we derived, we investigate the system performance of cellular systems adopting adaptive modulation and analyze the impacts of Nakagami fading and log-normal shadowing.

The results have been published in *Proc. PIMRC'2003* [66].

Chapter 5

In transmitter power allocation in MIMO systems, it is necessary to take practical considerations on discrete constellation sizes and the target BER performance. In this chapter, we analyze and reveal the underlying idea of the optimal power allocation strategy — Hughes-Hartog (H-H) algorithm [37]. Then we introduce a new index, so-called *power-increment-to-throughput-improvement ratio* (PITIR). Based on the new index, we derive and propose a novel suboptimal power allocation algorithm. The proposed algorithm is simpler and easier to implement, while it can achieve almost the same performance as the H-H algorithm in terms of the achievable data throughput and the power efficiency. Moreover, by utilizing the results obtained in the previous power allocation, the proposed algorithm can avoid unnecessary computation in the subsequent allocations. This means that the total computation complexity can be further reduced.

The results have been accepted for publication in *ISSSTA'2004* [67].

1.4 Thesis Outline

This thesis contains 6 chapters. In this chapter, we have introduced the studied problems and previous work. In Chapter 2, background knowledge is reviewed. In Chapter 3, we consider the problem of minimizing the outage probability in interference-limited Nakagami channels. New upper and lower bounds are derived for the outage probability. Consequently, we propose a new

power control algorithm, and show that the power solution can be obtained from solving the eigenvalue problem. In Chapter 4, we evaluate the system performance of interference-limited cellular systems adopting adaptive modulation. The approximate expression for the PDF of the received SIR is derived, where Nakagami fading and log-normal shadowing are considered. Then, the numerical results are presented. In Chapter 5, we study the optimal power allocation strategy in rate adaptive MIMO system. A novel sub-optimal algorithm is proposed, which achieves almost the same throughput performance and power efficiency as the optimal strategy with a reduced computation complexity. The thesis is concluded in Chapter 6.

Chapter 2

Background

2.1 Wireless Communication Systems

Ever since Guglielmo Marconi, in 1897, first demonstrated the possibility of the communications with ships sailing the English channel over the air, wireless communications has been widely recognized by people as a major communicating method. Particularly in the last years, the increasing demands of wireless services and applications and the tremendous research progress on communications technologies have significantly fueled the growth of wireless communications.

In comparison of the traditional wireline communications, wireless communications adopts the air as the transmission medium and provides people with the greatest flexibility during the communicating process. The fixed wireline communications is impossible to serve people who are moving. And in remote areas, cable installations are too costly. Therefore, mobility and accessibility supports are two main attractive characteristics of wireless communications.

However, the time-varying air channel makes the performance of wireless

communications technology unreliable. To make up such an impairment, sophisticated schemes applied to the whole communicating process greatly increase the cost of wireless communications services. As a result, modern communication system often combines both wireline and wireless communications to achieve a tradeoff among the performance, flexibility and cost.

2.1.1 Multiple Access Techniques

A basic issue concerned in the communication system design is to determine how to share the common radio spectrum among multiple users, i.e., the multiple access technique. The performance of the multiple access technique is of significance to the whole system and all the users, thus, researchers are always trying to find more efficient multiple access scheme.

Three well-known multiple access techniques are introduced here:

- *Time Division Multiple Access* (TDMA)

  In TDMA, the whole available transmission time is divided into frames. Each frame is then divided into time slots, and different time slots are assigned to different user upon request. During one time slot, the corresponding user can use up the whole available spectrum for transmission.

- *Frequency Division Multiple Access* (FDMA)

  In FDMA, the whole available spectrum is divided into several orthogonal channels with different frequencies. Each user is assigned a unique channel for transmission, and the channel will not be available to any other users

during the whole transmission time of its assigned user.

- *Code Division Multiple Access* (CDMA)

  Unlike TDMA and FDMA, a set of signature codes is employed in CDMA to separate users. For each user, the signature code is unique, therefore, divisions of spectrum or transmission time are not necessary in CDMA.

Usually in real system, hybrid schemes are adopted to improve the multiple access system's performance. For example, using FDMA, the whole spectrum can be divided into frequency channels, and then, each channel can be utilized in the way of TDMA or CDMA. The well-known second generation communication system GSM applies the combination of TDMA and FDMA.

2.1.2 Cellular Radio Systems

The radio spectrum is the most expensive resource in the system. When a large number of users are active in the system, the limited radio spectrum may hurt the system performance. Therefore, the concept of cellular system was initiated [71], which intends to reuse the frequency channels by separating them with enough geographical distance.

A common way to realize a cellular radio system is illustrated in Fig. 2.1. The area is divided into cells shaped as hexagons which will tessellate the service area. In each cell, a number of frequency channels are provided to support users. Channels in adjacent cells occupy different frequencies in order to minimize the interference from the adjacent cells. That is, in Fig. 2.1, Cell A uses different

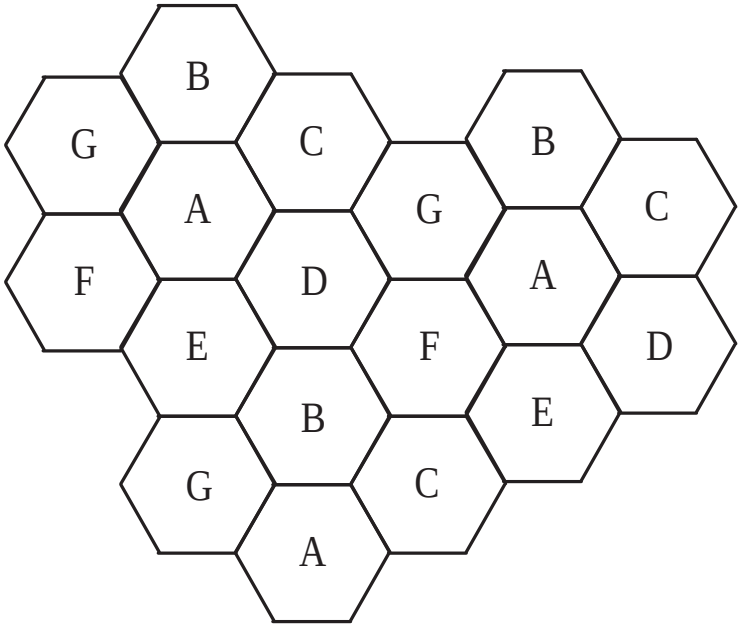

Figure 2.1: An illustration of cellular radio system.

frequency resource from Cell B, C, $\cdots$, and G. A group of cells that use up all available frequency spectrum is called a *cluster*, i.e., cells A, B, $\cdots$, and G form one cluster. The allocated full radio spectrum for the system is then reused in different clusters.

Though frequency reuse can increase the system capacity, it results in the interference that is harmful to the system performance. In cellular radio system, signals can be disturbed by the interference from the users using the same frequency in other cells, which is called *co-channel interference*. The corresponding cells are called *co-channel cells*. In Fig. 2.1, the users in cell A suffer from the interference from surrounding cells that are also labeled by A. Interfering cells are divided into *tiers* according to their distance to cell A. Six of them are the

nearest with approximately the same distance to cell A, which form the first tier; in the remaining interfering cells, twelve are the next nearest, which constitute the the second tier, $\cdots$, and so on. Generally, the interference from two tiers are considered in system design as other tiers are far away and result in a negligible interference.

2.1.2.1 Interference-limited Cellular System

When the interference is sufficient large and the noise is comparatively small to be negligible, the interference becomes the domination source determining the receiver performance. Such a system is known as *interference-limited* system.

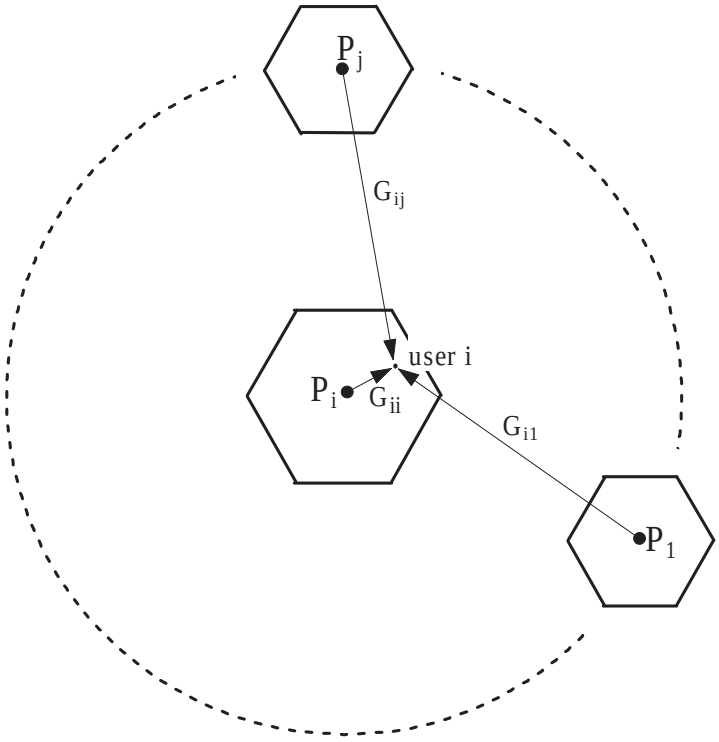

Figure 2.2: An illustration of interference-limited system model.

A simplified downlink model of the interference-limited cellular system is given in Fig. 2.2. There are N co-channel transmitters in total. Transmitter i is desired to serve user(receiver) i. Denote the transmitted power from transmitter i by P_i. Then the instantaneous received *signal-to-interference ratio* (SIR) of user i, SIR_i, is given by

$$\mathrm{SIR}_i = \frac{G_{ii}\alpha_{ii}^2 P_i}{\sum\limits_{j\neq i} G_{ij}\alpha_{ij}^2 P_j}\,, \tag{2.1}$$

where $P_i \geq 0$ for $i = 1, 2, \cdots, N$. G_{ij} and α_{ij} represent, respectively, the path gain (not include fading) and fading gain from transmitter j to receiver i. By assuming $E[\alpha_{ij}^2] = 1$, the average received SIR is given by

$$\overline{\mathrm{SIR}}_i = \frac{G_{ii}P_i}{\sum\limits_{j\neq i} G_{ij}P_j}\,. \tag{2.2}$$

The large-scale path loss process modeled by G_{ij} and the short-term fading process modeled by α_{ij} are described in Section 2.2.

2.1.3 MIMO Channel

The demand for capacity in wireless communication systems has grown significantly during the last decade. One major technological breakthrough that will meet this demand is the implementation of multiple antennas at the transmitter and receivers in the system. A system with multiple transmit and receive antennas is called a *multiple-input multiple-output* (MIMO) system.

A MIMO channel model is illustrated in Fig. 2.3. There are N_T transmit

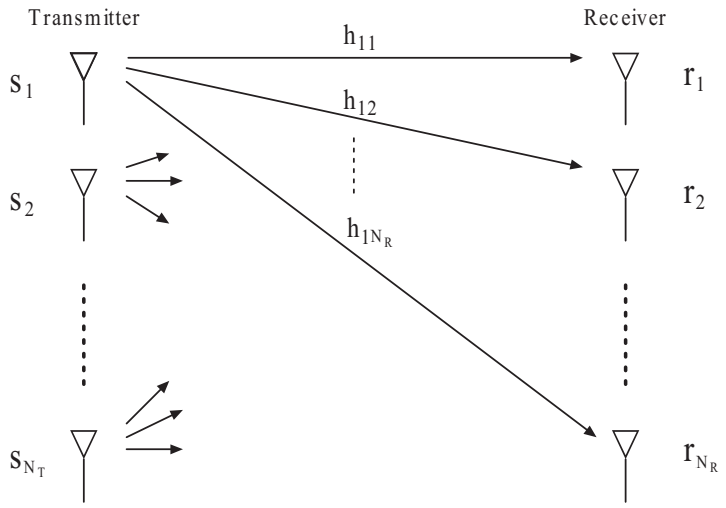

Figure 2.3: A MIMO channel with N_T transmit and N_R receive antennas.

and N_R receive antennas in the system. Let h_{ij} denote the complex channel gain between transmit antenna j and receive antenna i. We define the following $N_R \times N_T$ channel gain matrix,

$$\mathbf{H} = \begin{bmatrix} h_{11} & \dots & h_{1N_T} \\ \vdots & \ddots & \vdots \\ h_{N_R1} & \dots & h_{N_RN_T} \end{bmatrix}. \tag{2.3}$$

In this thesis, we assume that the channel between antennas is frequency flat. Therefore, no *inter-symbol interference* (ISI) occurs. Then we have

$$\mathbf{r} = \mathbf{H}\mathbf{s} + \mathbf{n} \tag{2.4}$$

where $\mathbf{s} = [s_1 \cdots s_{N_T}]^T$ and $\mathbf{r} = [r_1 \cdots r_{N_R}]^T$ are, respectively, the $N_T \times 1$

transmitted signal vector and the $N_R \times 1$ received signal vector. The $\mathbf{n} = [n_1 \cdots n_{N_R}]^T$ is an $N_R \times 1$ complex *additive white Gaussian noise* (AWGN) vector, with independent elements of identical power σ_N^2.

As the elements of the matrix $\mathbf{H}$ correspond to the complex channel gains between the transmit and receive antennas, a statistical distribution is usually postulated on the elements. In this thesis, we will assume that the elements of the channel gain matrix $\mathbf{H}$ is complex Gaussian random variables with zero mean and unit variance. Therefore, the magnitude of the channel gain $\mid h_{ij} \mid$ has a Rayleigh distribution. Meanwhile, we also assume in this thesis that the elements of $\mathbf{H}$ are statistically independent of each other for the simplicity. The model of $\mathbf{H}$ taking the fading correlation into account is studied in [72] and [73].

When $N_T = 1$ and $N_R > 1$, MIMO system reduces to *single-input multiple-output* (SIMO) system; when $N_T > 1$ and $N_R = 1$, MIMO system reduces to MISO system; when $N_T = N_R = 1$, MIMO systems reduces to *single-input single-output* (SISO) system.

2.2 Wireless Propagation Channel

In this section, we discuss large-scale path loss and small-scale fading which degrade the performance of wireless communication system.

2.2.1 Large-scale Path Loss

Large-scale path loss is often used to model the variation of the signal strength over the large transmitter-receiver separation. Such a variation is generally slow in time, which is thereby called *long-term fading* as well. There are two main models in this category [30].

- Log-distance Path Loss

  Both theoretical and measured results in the literature have shown that the signal power decreases logarithmically with the distance from the transmitter. Such a relationship can be expressed mathematically as

$$P_r(d) \propto P_t \cdot \left(\frac{1}{d}\right)^{\beta}, \tag{2.5}$$

  where $P_r(d)$ is the average received signal power at distance d from the transmitter, P_t is the transmitter power, and β is the pass loss exponent, the value of which depends on the specific propagation environment. Typical values of β can be found in [74].

  When a reference point is selected, $P_r(d)$ also follows the below expression,

$$P_r(d) = P_r(d_0)\left(\frac{d_0}{d}\right)^{\beta}, \tag{2.6}$$

  where d_0 and $P_r(d_0)$ are the distance from the transmitter to the reference point and the received signal power measured at the reference point, respectively. d_0 is commonly set to 1 km in macrocellular systems, and

much smaller (100 m or 1 m) in microcellular systems.

There are also several empirical path loss models developed for macrocellular or microcellular systems. A brief introduction to these models can be found in [70].

- Log-normal Shadowing

  Due to the surrounding clusters on the propagation path, the measured received signal may be different from the value predicted by (2.6). This phenomenon is specified as *shadowing*. Previous research has shown that the received signal (measured in dB) has a Gaussian (Normal) distribution with the mean equal to the value given by (2.6), which is the meaning of the term *log-normal*. Consequently, we obtain the (PDF) of the measured signal strength in dB as below

$$f(x_{dB}) = \frac{1}{\sqrt{2\pi}\xi} \exp\left(-\frac{(x_{dB} - P_{r_{dB}})^2}{2\xi^2}\right), \tag{2.7}$$

  where $P_{r_{dB}}$ is the value in dB of $P_r(d)$ that is given by (2.6). ξ is known as the *shadowing factor* of log-normal shadowing, which is determined according to the specific propagation environment.

2.2.2 Small-scale Fading

The presence of reflecting objects and scatters creates several possible transmitting paths for signal. Signal traveling in multiple paths generates several

copies of itself that arrive the receiver at the different time and could be different from the original one. Multipath signals interfere each other at the receiver, which results in the small-scale fading of signal as saw by the receiver. Unlike large-scale path loss which describes the variation of the average signal power over a long distance or time period, small-scales effects characterize the rapid fluctuation of the amplitude of the signal over a short distance or time period.

Multipath delay spread and Doppler spread are two important parameters for mobile multipath channel. Delay spread is resulted from the multipath transmission of signal, and Doppler spread is due to the mobile speed or the movement of surrounding objects. According to the relation between these two channel parameters and the signal parameters, two independent cataloging mechanisms are set up. The type of the fading is said to be frequency-selective fading or flat fading based on delay spread, while it is said to be fast fading or slow fading based on Doppler spread [74].

To describe the rapid time variation of the amplitude of the flat fading signal or an individual multipath component, several fading distribution models have been proposed, such as Rayleigh, Ricean and Nakagami distribution model.

- Rayleigh fading distribution

  In scattering environments, the composite received signal consists of a large number of plane waves, each of which can be treated as a complex Gaussian random process $\varrho(t) = \varrho_I(t) + j\varrho_Q(t)$. The envelop of the received signal obeys Rayleigh fading distribution if $\varrho_I(t)$ and $\varrho_Q(t)$ are

independent identically distributed zero-mean Gaussian random variables. In Rayleigh fading environments, the received signal has no *line-of-sight* (LoS) components.

The PDF of the signal envelop $r = \sqrt{\varrho_I^2 + \varrho_Q^2}$ is given by

$$f(r) = \frac{2r}{\Omega} \exp\left(-\frac{r^2}{\Omega}\right) \qquad r \geq 0\,, \tag{2.8}$$

where $\Omega = E[r^2]$, is the average received signal power. The corresponding cumulative distribution function (CDF) of r is given by

$$F(R) = \int_0^R f(r)dr = 1 - \exp\left(-\frac{R^2}{\Omega}\right)\,. \tag{2.9}$$

- Ricean fading distribution

  Compared to the case in Rayleigh fading environments, the received signal has a specular of LoS components. In this case, $\varrho_I(t)$ and $\varrho_Q(t)$ are Garssian random processes with non-zero means $\eta_I(t)$ and $\eta_Q(t)$.

  The PDF of the signal envelop $r = \sqrt{\varrho_I^2 + \varrho_Q^2}$ is given by

$$f(r) = \frac{2r}{\Omega} \exp\left(-\frac{r^2 + A^2}{\Omega}\right) I_0\left(\frac{2Ar}{\Omega}\right) \qquad A \geq 0,\ r \geq 0\,, \tag{2.10}$$

  where $A^2 = \eta_I^2 + \eta_Q^2$ denotes the average power of the LoS carrier, $I_0(\cdot)$ is the modified Bessel function of the first kind and zero-order, and Ω is the average received signal power.

A parameter K, known as the Ricean Factor, is often used to completely specify the Ricean distribution. It is defined as

$$K = \frac{A^2}{\Omega} . \tag{2.11}$$

It is well-known that when $K = 0$, the Ricean distribution reduces to the Rayleigh distribution. Thus, Ricean distribution is a more general channel fading model compared to Rayleigh distribution.

- Nakagami fading distribution

  In [75], Nakagami summarized the principal results of a series of statistical studies on the intensity distributions due to rapid fading and described a new fading channel model - Nakagami-m fading distribution. For simplicity, we will omit mentioning m in the later part of this thesis.

  Nakagami-m distribution is essentially a Chi-Square distribution. That is, for a signal experiencing Nakagami fading, the PDF of its envelope r is given by

$$f(r) = \frac{2m^m r^{2m-1}}{\Omega^m \Gamma(m)} \exp\left(-\frac{mr^2}{\Omega}\right) , \quad r \geq 0 \tag{2.12}$$

  where

$$m = \frac{\Omega^2}{E\left[(r^2 - \Omega)^2\right]} \tag{2.13}$$

$$\Omega = E\left[r^2\right] . \tag{2.14}$$

The constant parameter $m \geq \frac{1}{2}$ is the Nakagami-m fading parameter (also known as fading index or fading figure in different context), Ω is the average received power of the signal and $\Gamma(\cdot)$ is the Gamma function [76].

As shown in [75], the fading parameter m has a very important meaning in Nakagami fading distribution:

1) $m = \frac{1}{2}$, Nakagami distribution gives one-sided Gaussian distribution;

2) $m = 1$, Nakagami distribution degenerates to Rayleigh distribution;

3) $m = \infty$ corresponds the non-fading situation;

4) $1 < m < \infty$, Nakagami distribution approximates the Rice distribution, with the mapping function between m and K given by

$$m = \frac{(K+1)^2}{2K+1}\,. \tag{2.15}$$

Correspondingly, the instantaneous signal power p follows Gamma distribution, whose PDF is given by

$$f(p) = \left(\frac{m}{\Omega}\right)^m \frac{p^{m-1}}{\Gamma(m)} \exp\left(\frac{m}{\Omega}p\right)\,. \tag{2.16}$$

Chapter 3

Power Control for Minimum Outage in Interference-Limited Nakagami Fading Wireless Channels

Power control is of fundamental importance in the design of high capacity cellular radio systems. It is a crucial strategy to reduce co-channel interference caused by frequency reuse in cellular systems, and to alleviate the near-far problem in CDMA systems, in order to improve the performance and capacity of multiuser wireless systems. Two general categories of power control schemes in wireless systems are the centralized and the distributed schemes (refer to Chapter 1). These power control schemes require the receivers to know the instantaneous channel link gains or SIR of system users. Ideally, such schemes

have to be able to adapt to the fast changes of fading statistics, which could involve intensive computation and may not be easily realizable, especially when the number of system users is large.

In [68], Kandukuri and Boyd proposed a power control scheme for Rayleigh fading channels, which updates the transmitted powers of system users based on the relatively much longer time scale of shadowing, instead of the smaller time scale of fading. They showed that optimal power control in Rayleigh channels for minimizing outage probability can be approximately achieved by maximizing a parameter so-called the *certainty-equivalent margin* (CEM).

However, at present, no such power control algorithm for Nakagami fading channels have been published. In this chapter, we derive and study a new optimal power control algorithm for balancing outage probability in interference-limited Nakagami channels. We assume that all the desired signal and interferers are subject to non-identical and independent Nakagami fading, which is a general fading model that can model different fading environments. The Nakagami distribution [75] has been shown to have better flexibility and accuracy in matching some measurement data than the Rayleigh, Rician or log-normal distributions. From this viewpoint, our proposed scheme and results are very useful and include a result in [68] as a special case.

This chapter is organized as follows. In Section 3.1, we present the distribution models for the signal and interferers in Nagakami channels. In Section 3.2, by using an approximate PDF for a sum of interferers, we derive a relatively

simple expression of outage probability for Nakagami channels. In Section 3.3, we obtain tight upper and lower bounds for the outage probability to establish the validity of using a parameter, so-called *signal-to-interference ratio margin* (SIRM), as a new performance index in power control. In Section 3.3, we show that the new performance index provides us a more general theory and interpretation on power control problem in Nakagami fading channels, which helps us to see previous results in [68] and [5] in a more general perspective. Based on the criteria of balancing outage probability, we propose a new power control algorithm and show that optimal power control in Nakagami fading channels can be approximately achieved by SIRM balancing. Computation results are presented and discussed in Section 3.5.

3.1 System and Channel Models

Consider a cellular system consisting of a fixed number of independent channels that may be assigned to mobile users. Assume that a given channel is concurrently being used by N different links or transmitter-receiver pairs. Let $\mathbf{G} = \{G_{ij}\}$ denote the $N \times N$ path gain matrix, where G_{ij} is defined as the path gain (not including fading) from the jth transmitter to the ith receiver. The G_{ij} could model the path loss, log-normal shadowing, or cross correlations between codes in a CDMA system. We use r_{ij} to represent the envelope of the received signal at the ith receiver from the jth transmitter. Since r_{ij} is subjected to Nakagami fading, the instantaneous power $X_{ij} = r_{ij}^2$ is distributed

with the Gamma PDF [75]

$$f_{X_{ij}}(x) = \left(\frac{m_{ij}}{\Omega_{ij}}\right)^{m_{ij}} \frac{x^{m_{ij}-1}}{\Gamma(m_{ij})} \exp\left(-\frac{m_{ij}}{\Omega_{ij}}x\right) \tag{3.1}$$

where $\Gamma(\cdot)$ is the Gamma function, and m_{ij} is the fading severity index. The Ω_{ij} is the average received signal power defined as

$$\Omega_{ij} = E[X_{ij}] = G_{ij}P_j$$

where P_j denotes the average transmitted power at the transmitter j, and $E[\cdot]$ is the expectation operator.

For simplicity, we assume that all G_{ij}'s are constant, i.e. they do not change significantly over each power control interval. Therefore, our analysis throughout this paper holds for a time scale over which various factors that affect G_{ij} are approximately constant. We shall also ignore the effect of white noise in this work since it is negligible in interference-limited systems.

At the ith receiver, the sum of power from $N-1$ interferers is given by

$$Y_i = r_i^2 = r_{i1}^2 + r_{i2}^2 + \cdots + r_{i\,i-1}^2 + r_{i\,i+1}^2 \cdots + r_{i\,N-1}^2$$

where $r_{ij}\,(j \neq i)$ are Nakagami-distributed interferers. According to [75], r_i is approximately having the Nakagami distribution with (equivalent) fading

severity index M_i and average power I_i given by

$$\begin{aligned} M_i &= \left(\sum_{i\neq j} \Omega_{ij}\right)^2 \Big/ \sum_{i\neq j} \left({\Omega_{ij}}^2/m_{ij}\right) \\ I_i &= \left(\sum_{i\neq j} \Omega_{ij}\right) \end{aligned} \tag{3.2}$$

Equation (3.2) means that for any desired user, the statistics of a sum of Nakagami-faded interferers can be modeled approximately as a single Nakagami distributed interferer with parameters M_i and I_i. As to be shown later, the parameter M_i is to play a significant role in our analysis and derivation of the proposed algorithm.

The aggregate interference Y_i also has the Gamma distribution with parameters M_i and I_i,

$$f_{Y_i}(y) = \left(\frac{M_i}{I_i}\right)^{M_i} \frac{y^{M_i-1}}{\Gamma(M_i)} \exp\left(-\frac{M_i}{I_i}y\right). \tag{3.3}$$

In theory, M_i in (3.3) is a real number. However, in our later analysis and derivation, we shall use the nearest integral value of M_i. In practice, such an approximation is commonly used and acceptable due to several reasons [77]. Thus, from now on, when we mention M_i, we refer to its nearest integral value.

Next, (3.3) will be used to derive a relatively simple analytical formula of outage probability, with a negligible penalty on the accuracy.

3.2 Outage Probability Formula and Its Application

We assume that the QoS requirement is achieved when the SIR exceeds a given protection ratio or threshold ς_i. Otherwise, signal outage will occur. The outage probability at the ith receiver is specified as

$$\begin{aligned} P_i^{out} &= \text{Prob}\left(X_i/Y_i < \varsigma_i\right) = \text{Prob}\left(Y_i > X_i/\varsigma_i\right) \\ &= \int_0^\infty f_{X_i}(x) \int_{\frac{x}{\varsigma_i}}^\infty f_{Y_i}(y)\, dydx \end{aligned} \tag{3.4}$$

where X_i and Y_i are the instantaneous powers of the desired signal and the sum of interferers, respectively, with Gamma distribution defined in (3.1) and (3.3).

Define $\rho_a = \frac{M_i}{I_i} y$. According to [78], we have

$$\begin{aligned} \int_{\frac{x}{\varsigma_i}}^\infty f_{Y_i}(y)\, dydx &= \frac{1}{\Gamma(M_i)} \int_{\frac{xM_i}{\varsigma_i I_i}}^\infty \rho_a^{M_i-1} e^{-\rho_a} d\rho_a \\ &= \sum_{k=0}^{M_i-1} \frac{\left(\frac{xM_i}{\varsigma_i I_i}\right)^k}{k!} \exp\left(-\frac{xM_i}{\varsigma_i I_i}\right) \end{aligned} \tag{3.5}$$

Substituting (3.5) into (3.4), we get

$$P_i^{out} = \sum_{k=0}^{M_i-1} \left(\frac{m_{ii}}{\Omega_{ii}}\right)^{m_{ii}} \cdot \frac{1}{\Gamma(m_{ii})} \cdot \frac{\left(\frac{M_i}{\varsigma_i I_i}\right)^k}{k!} \int_0^\infty x^{(m_{ii}+k-1)} e^{-\left(\frac{m_{ii}}{\Omega_{ii}} + \frac{M_i}{\varsigma_i I_i}\right)x} dx \tag{3.6}$$

Define $\rho_b = \left(\frac{m_{ii}}{\Omega_{ii}} + \frac{M_i}{\varsigma_i I_i}\right) x$. According to [79], we have

$$\begin{aligned}\int_0^\infty x^{(m_{ii}+k-1)} e^{-\left(\frac{m_{ii}}{\Omega_{ii}}+\frac{M_i}{\varsigma_i I_i}\right)x} dx &= \frac{1}{\left(\frac{m_{ii}}{\Omega_{ii}} + \frac{M_i}{\varsigma_i I_i}\right)^{m_{ii}+k}} \int_0^\infty \frac{\rho_b^{m_{ii}+k-1}}{e^{\rho_b}} d\rho_b \\ &= \frac{\Gamma(m_{ii}+k)}{\left(\frac{m_{ii}}{\Omega_{ii}} + \frac{M_i}{\varsigma_i I_i}\right)^{m_{ii}+k}} \end{aligned} \tag{3.7}$$

Note that $\frac{\Gamma(m_{ii}+k)}{\Gamma(m_{ii})k!} = \binom{m_{ii}-1+k}{k}$. Substituting (3.7) into (3.6), we can obtain the expression of outage probability as

$$P_i^{out}(M_i) = \sum_{k=0}^{M_i-1} \binom{m_{ii}-1+k}{k} (1 + \frac{\varsigma_i I_i m_{ii}}{\Omega_{ii} M_i})^{-k} (1 + \frac{\Omega_{ii} M_i}{\varsigma_i I_i m_{ii}})^{-m_{ii}} \tag{3.8}$$

In fact, an exact outage probability formula for Nakagami channels has been derived in [77], in which the fading severity index m_{ij}'s are all assumed to be integers. However, their exact expression is a relatively complex one for us to derive any useful power control algorithm. Instead, we shall use the approximate outage probability expression (3.8) to highlight the relationship between SIR requirements and outage probabilities for a set of users in a system, as well as to derive a new power control algorithm for Nakagami channels.

3.3 SIRM as a Performance Index for Power Control

In this section, we derive a new performance index, so-called *signal-to-interference ratio margin* (SIRM), for power control in Nakagami fading channels. The SIRM constitutes the core of our main contribution in this paper. We then derive the upper bound and the lower bound for the outage probability expression (3.8), and establish the validity of maximizing the SIRM in our proposed power control algorithm. We shall present in Section 3.4 the proposed power control scheme for minimizing the probability of outage in Nakagami fading channels.

3.3.1 Relation between SIRM and Outage Probability

For the reason that becomes evident shortly, we define the *signal-to-interference margin* for user i $(i = 1, \cdots, N)$ as

$$\mathrm{SIRM}_i = \frac{\Omega_{ii}}{\varsigma_i m_{ii} \sum\limits_{i \neq j} \Omega_{ij}} \tag{3.9}$$

Then, we re-write (3.8) as

$$P_i^{out}(M_i) = \sum_{k=0}^{M_i - 1} \binom{m_{ii} - 1 + k}{k} \frac{(\mathrm{SIRM}_i \cdot M_i)^k}{(1 + \mathrm{SIRM}_i \cdot M_i)^{m_{ii}+k}} \tag{3.10}$$

Obviously, for given M_i and m_{ii}, P_i^{out} is monotonically decreasing with SIRM_i, since increasing SIRM_i is equivalently increasing the received SIR which results in a decrease of the outage probability.

3.3.2 Upper and Lower Bounds of Outage Probability

We define the maximum and minimum values of m_{ij}, respectively, as

$$\begin{aligned} m_{max} &= \max_{i,j}(m_{ij}) \\ m_{min} &= \min_{i,j}(m_{ij}) \end{aligned} \tag{3.11}$$

Only the interferers' powers are involved in the derivations below, therefore, we have $i \neq j$ and $i, j = 1, \cdots, N$ for the subscript in Ω_{ij}, where N is the number of co-channel links.

By definition in (3.11), we have

$$\frac{\left(\sum \Omega_{ij}\right)^2}{\sum\left(\Omega_{ij}^2\right)} \cdot m_{\min} \leq M_i \leq \frac{\left(\sum \Omega_{ij}\right)^2}{\sum\left(\Omega_{ij}^2\right)} \cdot m_{\max} \tag{3.12}$$

It is well-known that

$$\left(\sum \Omega_{ij}\right)^2 = \sum\left(\Omega_{ij}^2\right) + \sum\left(\Omega_{ij}\Omega_{kl}\right), \tag{3.13}$$

where $(i-k)^2 + (j-l)^2 \neq 0$. Note that the second term on the right-hand side of (3.13) has $(N-1)(N-2)$ quadratic cross products, and $\Omega_{ij}\Omega_{kl} + \Omega_{ij}\Omega_{kl} \leq$

$\Omega_{ij}^2 + \Omega_{kl}^2$. Thus, we have

$$0 < \sum (\Omega_{ij}\Omega_{ij}) \leq (N-2) \sum \left(\Omega_{ij}^2\right). \tag{3.14}$$

From (3.12), (3.13) and (3.14), we obtain the upper and lower bounds for M_i

$$m_{\min} < M_i \leq L m_{\max} \tag{3.15}$$

where $L = N-1$ is the number of interferers. In practice, we can estimate m_{min} and m_{max} and treat them as constants as long as they remain approximately unchanged throughout the whole adaptation process. To derive the upper bound and lower bound, we shall consider the following two cases: i) $m_{ii} > 1$; ii) $m_{ii} = 1$, separately.

Case 1: $m_{ii} > 1$: Nakagami faded signal, arbitrarily faded interferers

With a smaller M_i, the approximate PDF (3.3) for the interference has a larger spread, which implies that the interference is more probable of fluctuating around its average power value. Therefore, given a Nakagami PDF for the signal, the probability that the interference power level is higher than the desired signal power will increase as M_i decreases. In other words, the outage probability of the desired user is monotonically decreasing function of M_i. In Fig. 3.1, we plot the outage probability versus M_i, while the other parameters are kept as constants. Obviously, the curve matches our above speculation very well. This observation has been highlighted in [80] as well.

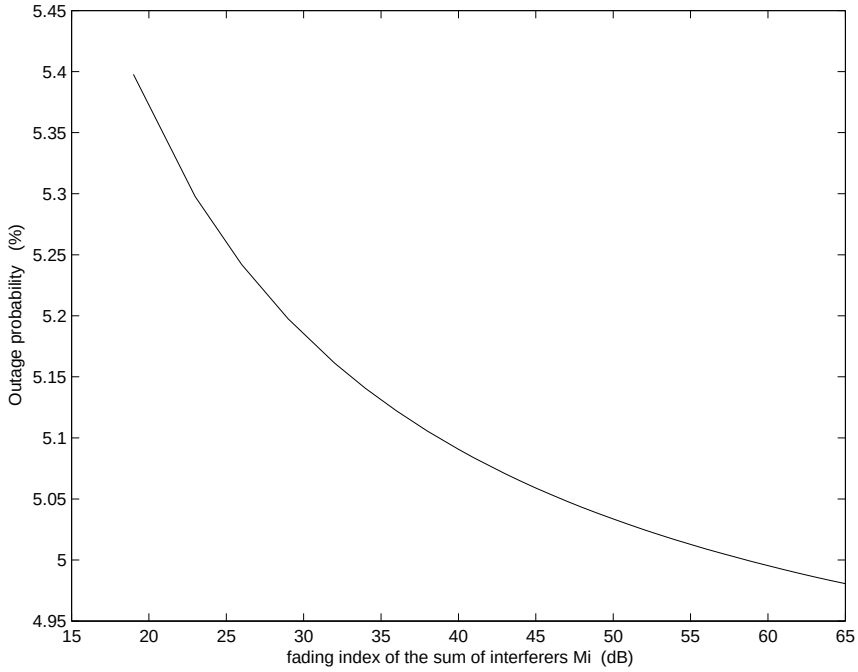

Figure 3.1: Outage probability versus fading severity index M_i for Nakagami channels with 4 users, $\boldsymbol{p}$=[30 50 40 55]; $\boldsymbol{m}$=[4 3 9 25]. The first user is assumed to be the desired user.

However, the above effect is obvious only when the average power of the desired signal is sufficiently stronger than the interference power, that is, when the SIR is sufficiently large. This is an assumption we shall use throughout this work, which is a commonly found scenario in practice.

Hence, for this case ($m_{ii} > 1$) we get

$$P_{L,i}^{out} \leq P_i^{out}(M_i) < P_{U,i}^{out}, \tag{3.16}$$

where $P_{L,i}^{out} = P_i^{out}(Lm_{max})$ and $P_{U,i}^{out} = P_i^{out}(m_{min})$. We shall refer to $P_i^{out}(m_{min})$ and $P_i^{out}(Lm_{\max})$ as, respectively, the upper bound and the lower bound of the outage probability for user i. A plot of these bounds is presented in Fig. 3.2. The

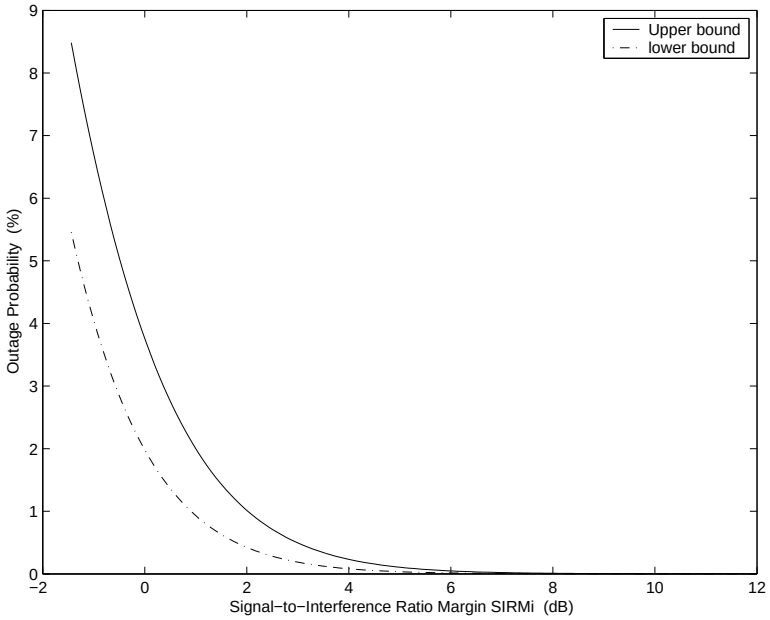

Figure 3.2: The upper and lower bounds of outage probability versus SIRM_i for Nakagami channels with 4 users, $\boldsymbol{p}$=[30 50 40 55]; $\boldsymbol{m}$=[4 3 9 25]. The first user is assumed to be the desired user.

lower and upper bounds are very close especially when the SIRM_i is sufficiently large.

Case 2: $m_{ii} = 1$*: Rayleigh faded signal, arbitrarily faded interferers*

When the desired signal is Rayleigh-faded (m_{ii}=1), the outage probability becomes larger as the equivalent fading parameter of the interference (i.e., M_i in this paper) increases. This is because with a larger M_i, the interference power is now more probable of maintaining at its average value; while the totally diffused desired signal (with $m_{ii} = 1$) is more randomly fluctuating and is therefore more probable of falling far below the interference power level. This observation has also been shown in [81].

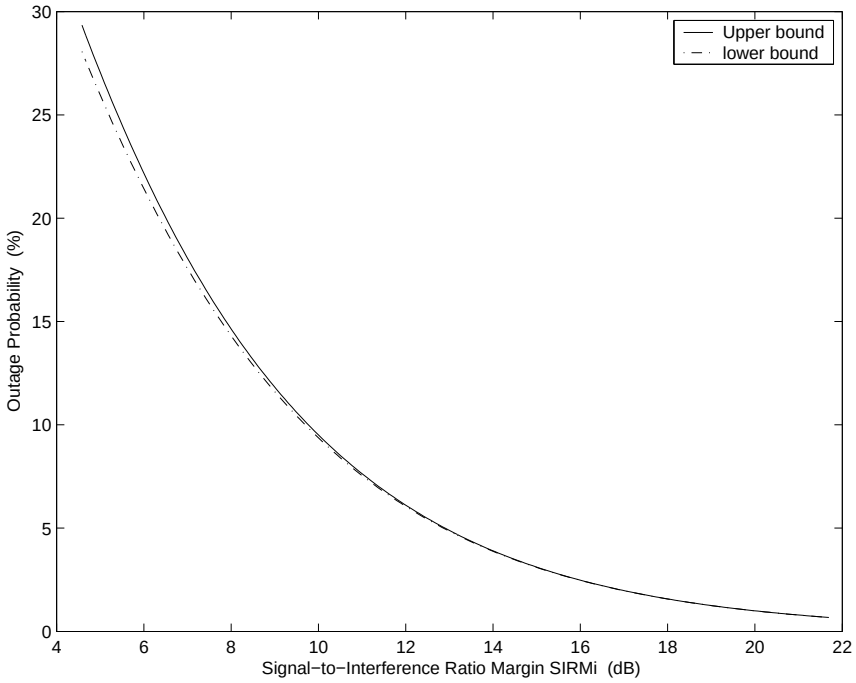

Figure 3.3: The upper and lower bounds of outage probability versus SIRM_i for Nakagami channels with 4 users, $\boldsymbol{p}$=[30 50 40 55]; $\boldsymbol{m}$=[1 3 9 25]. The first user is assumed to be the desired user.

By applying (3.15), we get,

$$P_{L,i}^{out} < P_i^{out}(M_i) \leq P_{U,i}^{out}, \tag{3.17}$$

where $P_{L,i}^{out} = P_i^{out}(m_{min})$ and $P_{U,i}^{out} = P_i^{out}(Lm_{max})$.

In contrast to *Case 1*, $P_i^{out}(m_{min})$ and $P_i^{out}(Lm_{max})$ are now, respectively, the lower bound and the upper bound of the outage probability for user i. In Fig. 3.3, we can see that the upper and lower bounds are very close to each other and the difference between them becomes insignificant as SIRM_i increases.

For the special case when all the signal and interferers are Rayleigh-distributed,

that is, $m_{ij} = 1$ for all i and j, we obtain the lower bound for the outage probability which is identical to the expression in [68, eq. (7)].

To summarize, the upper and lower bounds of the outage probabilities of each user i are both decreasing with SIRM_i and these bounds becomes closer to each other as SIRM_i increases. This is intuitively pleasing, since it is sufficient to maximize SIRM_i, in order to minimize the outage probability of user i. Next, we want to make use of the SIRM_i to develop an approximate optimal power control scheme based on the outage probability requirements.

3.3.3 Further Notes on Application of the Proposed Bounds

Recently, the problem of minimizing transmitter power with outage probability constraints is investigated in [82]. The authors employ jointly power control and linear multiuser detection to solve the power control problem in the uplink of CDMA system. By making use of the double conditioning property and Jensen's inequality, they develop an upper bound for the outage probability in Nakagami fading channels with Gaussian noise. They show that for each user, an upper bound for outage probability $\widetilde{P}_i^{out}$ can be written as

$$\widetilde{P}_i^{out} \leq \Gamma\left(\frac{m_{ii}}{CEM_i^{\sigma}}, m_{ii}\right) \tag{3.18}$$

where $\Gamma(x,a) = \frac{1}{\Gamma(a)} \int_0^x e^{-t} t^{a-1} dt$, is the incomplete Gamma function, $CEM_i^{\sigma} = \frac{G_{ii}P_i}{\sum_{i \neq j} G_{ij}P_j + \sigma^2}$, where σ^2 is noise power in the channel. Note that $\widetilde{P}_i^{out}$ is slightly different from the definition in (3.4) which is for interference-limited system.

The results in [82] show that when $m_{ii} \leq 1$, the right-hand side of (3.18) behaves as a tight upper bound of the outage probability. By using the bound, the outage probability constraints considered are mapped to the constraints on the average SINR in [82]. This mapping allows the authors to develop a sub-optimal algorithm to solve the original power control problem. However, for $m_{ii} \geq 1$, the right-hand side of (3.18) is no longer valid to be used as an upper bound [82]. Instead, the authors claim that it should be treated as an approximation of $\widehat{P}_i^{out}$.

Here, we want to highlight that the upper bounds, (3.16) and (3.17), developed by us in Chapter 3.3.2 can also be used to map the outage probability constraints to the average SIR constraints. Thus, the bounds is applicable to the same problem in [82] for the case of interference-limited system with $m_{ii} \geq 1$.

3.4 Proposed Power Control Algorithm for Nakagami Fading Channels

Obviously, from (3.9), SIRM_i is monotonically increasing with the desired signal power P_{ii} and monotonically decreasing with interference power $P_{ij} (i \neq j)$. To optimize the overall system performance, we should consider maximizing

the SIRM for all users. As a result, all users will achieve an optimal SIRM value, that is, when and only when all SIRM_i are equal. A similar scheme has been discussed for Rayleigh fading channels in [68], in which the performance index CEM is optimized jointly for all users by solving this problem,

$$\begin{aligned} &\text{maximize} && \text{CEM} \\ &\text{subject to} && \frac{\Omega_{ii}}{\varsigma_i \sum_{i \neq j} \Omega_{ij}} = \text{CEM},\ i = 1, \ldots, n \\ & && P_i > 0,\ i = 1, \ldots, n \end{aligned} \tag{3.19}$$

We have noted that with the constraints $P_i > 0$, (3.19) is simply a balancing problem. Therefore, we shall use this simple criteria for balancing to achieve equal SIRM for all active users in our objective function. From this viewpoint, our result is also an generalization of the analysis in [68] to Nakagami fading channels.

Based on the above argument, the optimal power control problem can be simply formulated as a SIRM balancing problem, i.e.,

$$\frac{\Omega_{ii}}{\varsigma_i m_{ii} \sum\limits_{i \neq j} \Omega_{ij}} = u, \qquad i = 1, \ldots, n \tag{3.20}$$

where s is an arbitrary constant. Substituting (3.11) into (3.20) and by definition, $\Omega_{ij} = G_{ij} P_j$, the above optimization problem is equivalent to

$$\frac{\varsigma_i m_{ii} \sum_{i \neq j} G_{ij} P_j}{G_{ii} P_i} = v, \qquad P_i > 0,\ i = 1, \ldots, n \tag{3.21}$$

where v is an arbitrary constant.

Therefore, we can write the system equations (3.21) in matrix and vector form as

$$\mathbf{AP} = v\mathbf{P}, \qquad P_i > 0,\ i = 1, \ldots, n \tag{3.22}$$

where the matrix $\mathbf{A}$ consists of elements $A_{ij} = \frac{\varsigma_i m_{ii} G_{ij}}{G_{ii}}$ for $i \neq j$, and $A_{ii} = 0$.

Equation (3.22) is recognized as an eigenvalue problem for the matrix $\mathbf{A}$ with all nonnegative entries A_{ij}. The optimal power vector solution for the system users is unique and can be solved according to the Perron-Frobenius theory.

It is interesting to note that (3.22) is in a familiar form as in the case of SIR balancing [5]. However, it can be interpreted in a more general perspective, and therefore provides us a more general theory than all previous results. Since the matrix $\mathbf{A}$ in (3.22) is a function of the fading severity index m_{ii} as well as the average powers Ω_{ij} of all users, it actually takes into account the fading statistics in Nakagami fading. An implication of the above finding is: even when all users have identical average path gains, the distribution of total average power among the LOS and the diffused components still constitutes another important factor, which determines the level of power to be transmitted for maintaining a required outage probability. From this viewpoint, our result in (3.22) is more general than former formulation in [5] and other similar works, where only fixed channel gains are considered.

For the special case of $m_{ii} = 1$ for all i, the matrix $\mathbf{A}$ includes the average power of the Rayleigh fading, $\Omega_{ij} = G_{ij} P_j$, and reduces to exactly the same form

as [5]. However, the G_{ij} should be now interpreted as the resulting path gain after *averaging over channel fading*, which corresponds to previous formulation in [5] only if the G_{ij}'s are (approximately) constant during the observation period.

Therefore, we can view (3.22) as a more general formulation of the power control problem in Nakagami fading channels, and this constitutes one of our main contributions in this paper. Note that since the SIR thresholds ς_i could be distinct for each user, all our formulation and analysis above are valid for systems with either heterogenous SIR thresholds or homogenous SIR thresholds.

3.5 Numerical Results and Discussions

In this section, we present computation results to demonstrate and verify the above formulation and analysis. We consider a system with 15 transmitter-receiver pairs, with each wireless link being subjected to Nakagami fading. Note that we neglect the effect of white noise.

We set all channel gains G_{ii} (from ith transmitter to ith receiver) to be unity, and randomly generate the channel gain of the interferers, G_{ij}, $(i \neq j)$, as independent variables uniformly distributed between zero and 0.001. This parameter setting is used to obtain sufficient high SIR, which is of practical interest. We assume homogeneous SIR thresholds system with the SIR thresholds $\varsigma_i = \varsigma$ for all i, and vary ς from 5dB to 12dB.

The result in Fig. 3.4 refers to the case where at all signal and interferers

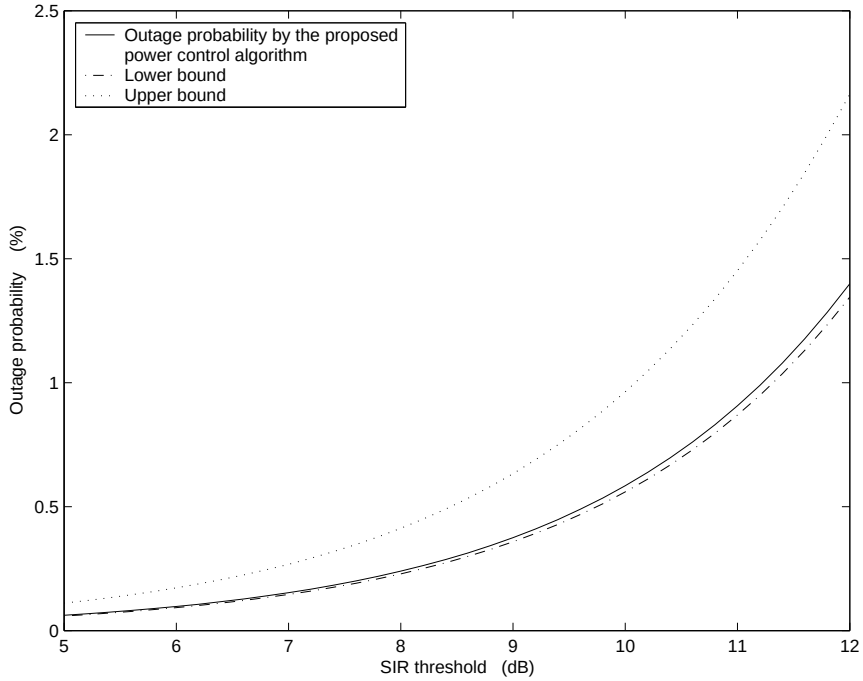

Figure 3.4: Outage probability in Nakgami fading channels obtained by the proposed power control algorithm, and the upper bound and lower bound versus SIR threshold ς, for a system with 15 users. The first user is assumed to be the desired user.

are subjected to Nakagami fading, i.e. $m_{ij} > 1$ for all j. The optimal power vectors $\mathbf{P}$ is obtained by solving (3.22) according to the Perron-Frobenius theory. The resulting outage probability lies between the upper and lower bounds (3.16), and in particular, is very close to the lower bound. As expected, the outage probability increases as the SIR threshold increases, since the SIRM is monotonically decreasing with the SIR threshold.

Finally, we want to emphasize that even though we have considered only the case of identical SIR thresholds for all users (homogeneous SIR thresholds systems), the above observations are also valid for heterogenous SIR thresholds systems with distinct SIR thresholds ς_i for every user.

3.6 Conclusion

We have derived and studied a new optimal power control scheme for interference-limited Nakagami channels, with the objective of balancing outage probability for a system of mobile users. We have highlighted and described the inherent relationship between the newly proposed performance index SIRM, the outage probability requirement, and the fading parameters of desired signal and interferers in Nakagami channels. We further show that it is feasible to maximize the SIRM to approximately achieve the objective of balancing outage probability, and this problem can be easily solved by using the Perron-Frobenius theory.

In the next chapter, we will evaluate the throughput performance of interference-limited adaptive modulation system in the presence of Nakagami fading and log-normal shadowing.

Chapter 4

Performance of Adaptive MQAM in Cellular System with Nakagami Fading and Log-normal Shadowing

Adaptive modulation is a critical technique to obtain spectrally efficient communication systems in slow-fading channels. Contrary to the non-adaptive modulation, it requires the accurate feed-back of the channel information at the transmitter so as to change the modulation scheme. When the channel is of good quality or when the interference is weak, which corresponds to a high SNR or a high SIR, higher order modulation may be used to achieve a higher average system throughput and vice versa, while maintaining a given target BER.

Previous efforts have shown that the adaptive modulation can efficiently improve the system throughput in wireless channels [83]. However, no results for Nakagami fading channels with log-normal shadowing have been reported in the literature, and moreover, the statistic of co-channel interference is often ignored in previous works. In this chapter, we study the performance of adaptive modulation over Nakagami fading channels with log-normal shadowing in an interference-limited system, where the constellation sizes are adapted according to the received SIR of each user.

To take into account the statistics of co-channel interference, we use a new approach to derive the expression for the PDF of the instantaneous received SIR. We approximate the composite Gamma-log-normal distribution as another log-normal distribution [70], and apply the previous results in [69] on the statistic of the sum of log-normal random variables. Based on the PDF of the SIR we obtained, we investigate the system performance of adaptive modulated cellular systems and the impacts of Nakagami fading and log-normal shadowing.

This chapter is organized as follows. In Section 4.1, we discuss the system and channel models under consideration. In Section 4.2, we derive the approximate expression of the PDF for the instantaneous SIR in cellular system with Nakagami fading and log-normal shadowing. The performance of the adaptive MQAM modulation is analyzed in Section 4.3. Numerical results are presented in Section 4.4, and some conclusion remarks are given in Section 4.5.

4.1 System and Channel Models

Consider the downlink of an interference-limited system where the thermal noise is assumed to be negligible. Let $\{U_i\}$, $\{B_i\}$ and $\{P_i\}$, $i = 1 \cdots N$, denote a set of co-channel users, their associated base stations and the corresponding transmitted powers at the base stations, respectively. Let r_{ij} represent the signal received by U_i from B_j, where r_{ij} is the desired signal if $i = j$; otherwise, it is the interference. We define $F_{ij} = d_{ij}^{-\beta}$ as the path loss gain of the link from B_j to U_i, where d_{ij} denotes the distance from B_j to U_i, and β denotes the path loss factor, which is assumed to be equal for all co-channel links in this work.

We assume all users' signals are subjected to independent Nakagami fading with log-normal shadowing. For the communication link from B_j to U_i, the instantaneous received signal power P_{ij}, can be written as

$$P_{ij} = {\alpha_{ij}}^2 10^{\xi_{ij}/10} F_{ij} P_j \tag{4.1}$$

where α_{ij} represents the Nakagami fading amplitude, and ξ_{ij} is known as the shadowing factor, and is a Gaussian random variable with zero mean and variance $\sigma_{\xi_{ij}}^2$.

The Nakagami distribution is a general fading channel model. It matches the Rayleigh distribution when fading severity index $m = 1$, and it approximates the Rician distribution when $m > 1$ with a simple function relating the Rician factor K and m [75]. It is well-known that $X = \alpha_{ij}^2$ is a Gamma random variable

with the PDF given by

$$f_X(x) = \left(\frac{m_{ij}}{\Omega_{ij}}\right)^{m_{ij}} \frac{x^{m_{ij}-1}}{\Gamma(m_{ij})} \exp\left(-\frac{m_{ij}}{\Omega_{ij}}x\right) \tag{4.2}$$

where $m_{ij} \geq 1/2$ is the fading severity index, and $\Omega_{ij} = E[{\alpha_{ij}}^2]$. $E[\cdot]$ is the expectation operator and $\Gamma(\cdot)$ is the Gamma function. In our later analysis, we assume m_{ij} to be an integer, which is acceptable in most practical applications.

4.2 Proposed PDF for Instantaneous SIR

To derive the PDF of instantaneous SIR, we shall first derive the PDF of the desired signal and the total interference separately.

4.2.1 Distribution of the Desired Signal

According to [70], $P_{ij}/(F_{ij}P_j)$, can be accurately approximated by a log-normal random variable. The equivalent shadowing factor λ_{ij} defined by

$$10^{\lambda_{ij}/10} = 10^{\xi_{ij}/10}\alpha_{ij}^2 \tag{4.3}$$

is approximately a Gaussian random variable with the mean $\eta_{\lambda_{ij}}$ and variance $\sigma^2_{\lambda_{ij}}$ given by

$$\begin{aligned} \eta_{\lambda_{ij}} &= \tfrac{1}{c}[\psi(m_{ij}) - \ln(m_{ij})] \\ \sigma^2_{\lambda_{ij}} &= \tfrac{\zeta(2,m_{ij})}{c^2} + \sigma^2_{\xi_{ij}} \end{aligned} \tag{4.4}$$

where $c = \ln(10)/10$. $\psi(\cdot)$ is the Euler psi function given by

$$\psi(\nu) = \sum_{i=0}^{\infty} \frac{1}{i} - C, \quad C \cong 0.5772 \tag{4.5}$$

where ν is a positive integer, and $\zeta(\cdot)$ is the Riemann's zeta function defined as

$$\zeta(2, \nu) = \sum_{i=0}^{\infty} \frac{1}{(\nu + i)^2}, \quad \nu \neq 0, -1, -2, \ldots \tag{4.6}$$

Therefore, the received power P_{ij} can be written as

$$P_{ij} = 10^{\lambda'_{ij}/10}, \tag{4.7}$$

where $\lambda'_{ij} = \lambda_{ij} + 10\log_{10}(F_{ij}P_j)$ is a Gaussian random variable with mean and variance, respectively, given by

$$\begin{aligned} \eta_{\lambda'_{ij}} &= \tfrac{1}{c}[\psi(m_{ij}) - \ln(m_{ij}) + \ln(F_{ij}P_j)] \\ \sigma^2_{\lambda'_{ij}} &= \tfrac{\zeta(2, m_{ij})}{c^2} + \sigma^2_{\xi_{ij}} \end{aligned} \tag{4.8}$$

The above approximation is valid for $\sigma_{\xi_{ij}} > 6$ dB for arbitrary integral value of m_{ij} [70].

4.2.2 Distribution of the Interference

It is well known that a sum of log-normal random variables can be approximated by another log-normal random variable with appropriately chosen distribution parameters. Hence, the total received interference of U_i is given by

$$I_i = \sum_{k=1,k\neq i}^{N} P_{ik} \approx 10^{\omega_i/10}, \tag{4.9}$$

where ω_i is a Gaussian random variable with mean η_{ω_i} and variance $\sigma^2_{\omega_i}$.

Schwarts-Yeh's methods [69] has been shown in [84] to be accurate in computing the moments of a sum of multiple log-normal random variables for the shadowing factor $\sigma_{\xi_{ij}}$ ranging from 6 to 12 dB, which is of practical interests. Thus, in this paper, we use Schwarts-Yeh's methods to compute the mean η_{ω_i} and the variance η_{ω_i} in (4.9).

Schwarts-Yeh's method is based on the derivation of the exact expressions for the mean and the variance of the sum of two log-normal random variables. Given two independent log-normal random variables denoted as X_1, X_2, we first define $Y_i = \ln(X_i)$, $i = 1, 2$. The sum of X_i, $i = 1, 2$, can be approximated by another log-normal random variable, with its natural logarithmic value denoted as Z. Thus, we have

$$Z = \ln(X_1 + X_2) = \ln(e^{Y_1} + e^{Y_2}) \tag{4.10}$$

We define $V = Y_2 - Y_1$, the mean and variance of Z are, respectively, given by

$$\begin{aligned} \eta_Z &= \eta_{Y_1} + g_1 \\ \sigma_Z^2 &= \sigma_{Y_1}^2 - g_1^2 - 2\sigma_{Y_1}^2 g_3 + g_2 \end{aligned} \tag{4.11}$$

where the functions g_1, g_2 and g_3 are given by

$$\begin{aligned} g_1 &= E[\ln(1 + e^V)] \\ g_2 &= E[\ln^2(1 + e^V)] \\ g_3 &= E[(V - \eta_V)\ln(1 + e^V)] \end{aligned} \tag{4.12}$$

For $n > 2$, the above procedure can be repeated to evaluate the corresponding mean and variance of the equivalent log-normal distribution in a nested fashion.

4.2.3 PDF of the Received SIR

The received SIR for the ith user is defined as $\gamma_i = P_{ii}/I_i$. Therefore, we obtain

$$\gamma_i = \frac{10^{\lambda'_{ii}/10}}{10^{\omega_i/10}} = 10^{z_i/10} \tag{4.13}$$

where $z_i = \lambda'_{ii} - \omega_i$.

In (4.13), both λ_{ii} and ω_i are Gaussian random variables, and hence, z_i is also a Gaussian random variables. If we define the correlation coefficient between

λ_{ii} and ω_i as $r_{\lambda'_{ii},\omega_i}$, the mean and variance of z_i are, respectively,

$$\begin{aligned} \eta_{z_i} &= \eta_{\lambda'_{ii}} - \eta_{\omega_i} \\ \sigma^2_{z_i} &= \sigma^2_{\lambda'_{ii}} + \sigma^2_{\omega_i} - 2r_{\lambda'_{ii},\omega_i}\sigma_{\lambda'_{ii}}\sigma_{\omega_i} \end{aligned} \tag{4.14}$$

Since λ_{ii} and ω_i, respectively, describe the statistics of the desired signal power and the total interference power approximately, for simplicity, we assume they are uncorrelated, i.e., $r_{\lambda'_{ii},\omega_i} = 0$.

Thus, the instantaneous received SIR, γ_i, for U_i in an interference-limited system has the log-normal distribution given by

$$f_{\gamma_i} = \frac{1}{c\sigma_{z_i}\sqrt{2\pi}\gamma_i} \exp\left(-\frac{\left(\ln(\gamma_i)/c - \eta_{z_i}\right)^2}{2\sigma^2_{z_i}}\right) \tag{4.15}$$

The average SIR $\overline{\gamma}_i$ can be evaluated as

$$\overline{\gamma}_i = E[\gamma_i] = e^{c\eta_{z_i} + \frac{1}{2}c^2\sigma^2_{z_i}} \tag{4.16}$$

4.3 Performance Criterions

We consider a set of N users in the system, given a target BER Υ. We shall adopt the adaptive MQAM scheme, where the constellation size for every user is chosen according to its SIR, and the constellation size is restricted to $S_j = 2^j$, $j = 1, 2, \cdots, s$.

The block diagram of a general adaptive MQAM modulation system is given

in Fig. 5.2. At the receiver, the SIR is measured, and constellation sizes are adapted according to the received SIR to improve the system throughput.

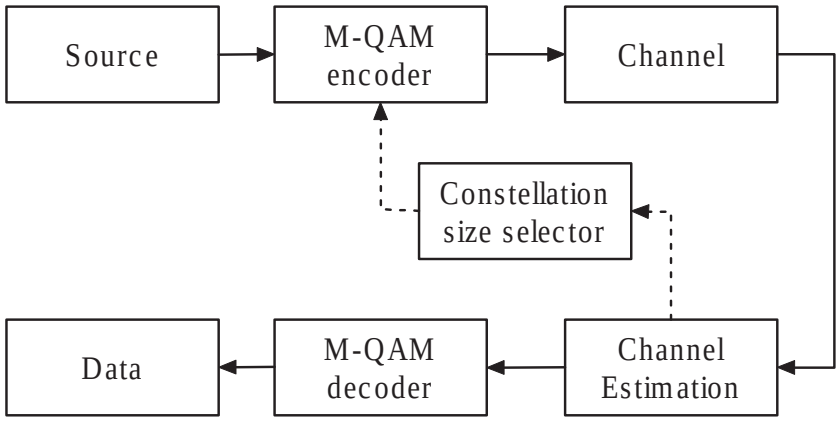

Figure 4.1: A general adaptive MQAM modulation system

4.3.1 Average Throughput per User

An approximate expression for BER of M-QAM modulation has been derived in [85] as,

$$\tau_{b,S}(\gamma) = \begin{cases} Q(2\gamma) & S = 2 \\ \frac{1-\left(1-F_{\sqrt{S}}(\gamma)\right)^2}{\log_2 S} & S = 2^{2n} \\ \frac{1-\left[1-2Q\left(\sqrt{\frac{3}{S-1}\gamma}\right)\right]^2}{\log_2 S} & S = 2^{2n+1} \end{cases} \tag{4.17}$$

where γ denotes the received SIR, n is an arbitrary positive integer, S denotes the modulation size, and $F_{\sqrt{S}}(\gamma)$ is given by

$$F_{\sqrt{S}}(\gamma) = 2\left(1 - \frac{1}{\sqrt{S}}\right) Q\left(\sqrt{\frac{3}{S-1}\gamma}\right). \tag{4.18}$$

Table 4.1: Constellation Size, Required SIR, and Throughput (Bits/Symbol) for Target BER of 10^{-3}

S	2	4	8	16	32	64
SIR (dB)	6.79	9.80	13.71	16.54	19.75	22.55
$\log_2 S$	1	2	3	4	5	6

Table 4.2: Constellation Size, Required SIR, and Throughput (Bits/Symbol) for Target BER of 10^{-6}

S	2	4	8	16	32	64
SIR (dB)	10.53	13.54	17.32	20.42	23.59	26.56
$\log_2 S$	1	2	3	4	5	6

The Q-function can be expressed in terms of error function as

$$Q(x) = \frac{1}{2} erfc\Big(x/\sqrt{2}\Big) \tag{4.19}$$

Given Υ, we can select the constellation size, S, of MQAM modulation for a specified user by substituting the received SIR to (4.17). In addition, we can also use (4.17) to decide the SIR threshold levels $\{\gamma_i^{th}, i = 1, 2, \cdots, s\}$ for switching the constellation size, given the Υ and the corresponding S. Unfortunately, it is difficult to obtain the analytical form of either the constellation size S as a function of Υ and SIR γ, or the switching levels of SIR $\{\gamma_i^{th}\}$ as a function of Υ and S. Therefore, for the given Υ, we shall use numerical search to obtain the switching levels $\{\gamma_i^{th}\}$ corresponding to the set of constellation size $\{S_j = 2^j,\, j = 1, \cdots, s\}$.

Let $T_u^{(i)}$ denote the throughput of user U_i, which is defined as the number of

bits that can be successfully transmitted to this user within each transmitted symbol. Note that $T_u^{(i)}$ is also the spectral efficiency for MQAM modulation, with unit of bits per second per Hertz of bandwidth. We have

$$T_u^{(i)} = \sum_{j=1}^{j=s} \log_2(S_j) Prob_i(S_j) \tag{4.20}$$

In (4.20), the $Prob_i(S_j)$ denotes the probability that the constellation size S_j is assigned to U_i, which is evaluated as

$$Prob_i(S_j) = \int_{\gamma_j^{th}}^{\gamma_{j+1}^{th}} f_{\gamma_i}(\gamma) d\gamma \tag{4.21}$$

where γ_j^{th} and γ_{j+1}^{th} are obtained, respectively, by substituting S_j and S_{j+1} into (4.17) for a given Υ. Note that $\gamma_{s+1}^{th} = \infty$.

Therefore, the average system throughput is given by

$$T_{av} = \frac{1}{N} \sum_{i=1}^{i=N} T_u^{(i)} \tag{4.22}$$

4.3.2 Average Outage Probability per User

We define that the outage occurs when no constellation size can achieve the given Υ for a user because of very low SIR, that is,

$$P_i^{out} = \int_0^{\gamma_1^{th}} f_{\gamma_i}(\gamma) d\gamma \tag{4.23}$$

where γ_1 is obtained by substituting $S_1 = 2$ and the value of Υ into (4.17).

The average outage probability is

$$P_{av}^{out} = \frac{1}{N} \sum_{i=1}^{i=N} P_i^{out} \tag{4.24}$$

4.4 Numerical Results and Discussions

In our computation, we consider an interference-limited cellular system in which each base station is located at the center of a cell. Without loss of generality, we take U_1 as the desired user, who is interfered by three co-channel interfering base stations B_j, $j = 2, 3, 4$, at the first tier, all with the same distance from U_1. Thus, by assuming that the path loss exponents are equal for each wireless link, we have $F_{1j} = F_I$, $j = 2, 3, 4$. It should be noted here that F_{11}/F_I is the magnitude of the area mean SIR. We will normalize F_{11} to 1 and change the value of F_I in below examples. We also set the transmitted powers at the each base station to unity.

Without loss of generality, we evaluate the average throughput and outage probability of user U_1 as the average system performance, since all users are equivalent following our system model. We assume identical variances $\sigma_{\xi_{ij}}^2$ for all users, which is reasonable because the standard deviation of log-normal shadowing mainly depends on the large-scale propagation characteristic.

The MQAM scheme with six constellation sizes S_j, $j = 1, 2, \cdots, 6$, is available

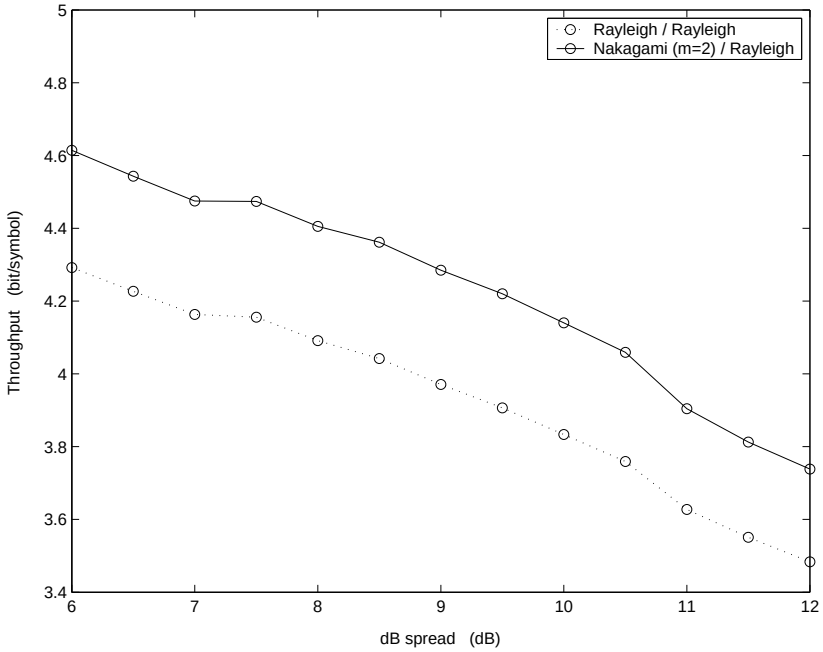

Figure 4.2: Average throughput of MQAM versus shadowing factor where the shadowing factor of the desired signal is set to 6 dB, while the shadowing factor of the interferers varies from 6 to 12 dB. The desired/interference signals are subjected to (i) Rayleigh fading/Rayleigh fading and (ii) Nakagami fading ($m = 2$)/Rayleigh fading, with each case represented by dotted line and solid line, respectively. $F_{11} = 1$, $F_I = 10^{-3}$.

for each user. By solving (4.17) numerically, we obtain the values of SIR switching levels for each constellation size for a given Υ. The results for $\Upsilon = 10^{-3}$ and $\Upsilon = 10^{-6}$ are tabulated in Table 4.1 and Table 4.2, respectively.

In Fig. 4.2, we show the average system throughput, computed using (4.20), versus the shadowing factor of interferers. We consider the case where the desired signal is subjected to (i) Rayleigh fading and (ii) Nakagami fading ($m = 2$). The shadowing factor of the desired signal is set to 6 dB, and along the x-axis, the shadowing factor of interferers is from 6 to 12 dB. We observe that when the desired signal is subjected to Rayleigh fading, the throughput performance is

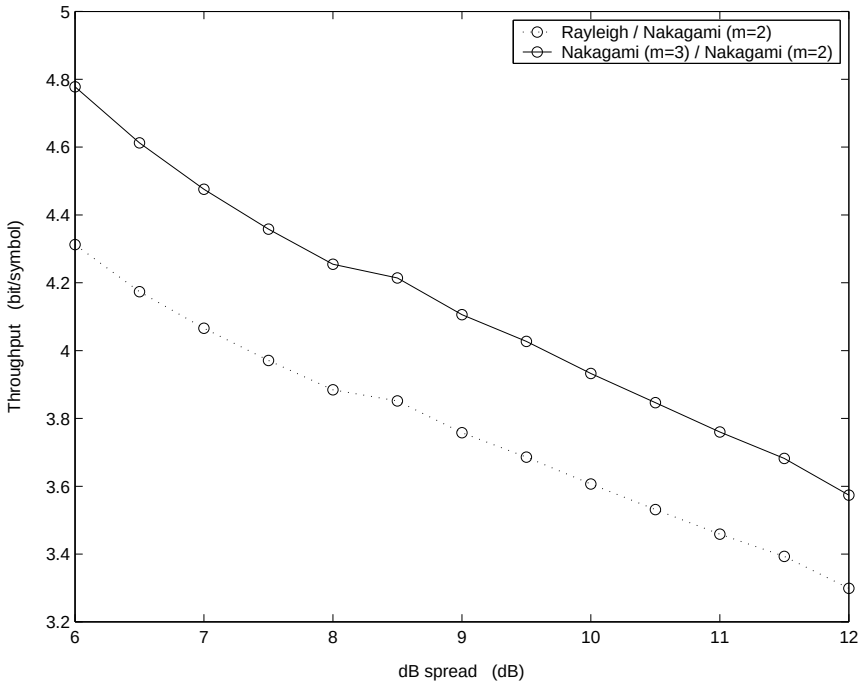

Figure 4.3: Average throughput of MQAM versus shadowing factor where the shadowing factor is identical for all users, which varies from 6 to 12 dB. The desired/interference signals are subjected to (i) Rayleigh fading/Nakagami fading ($m = 2$) and (ii) Nakagami fading ($m = 3$)/Nakagami fading ($m = 2$), with each case represented by dotted line and solid line, respectively. $F_{11} = 1$, $F_I = 10^{-3}$.

worse than the case of Nakagami fading. This is expected because the Rayleigh fading is a more severe fading condition than the latter. Another observation is that the throughput performance is better when the interferers have smaller shadowing factor. Similar trend is observed when we adjust the shadowing factor of all users at the same time from 6 to 12 dB, as shown in Fig. 4.3.

The outage probability is computed using (4.23) and is presented in Fig. 4.4, where the shadowing factor is identical for all users, which varies from 6 to 12 dB. As expected, the outage probability becomes larger when the desired signal is subjected to Rayleigh fading, which corresponds to more severe fading.

We study the average system throughput versus shadowing factor for $\Upsilon =$

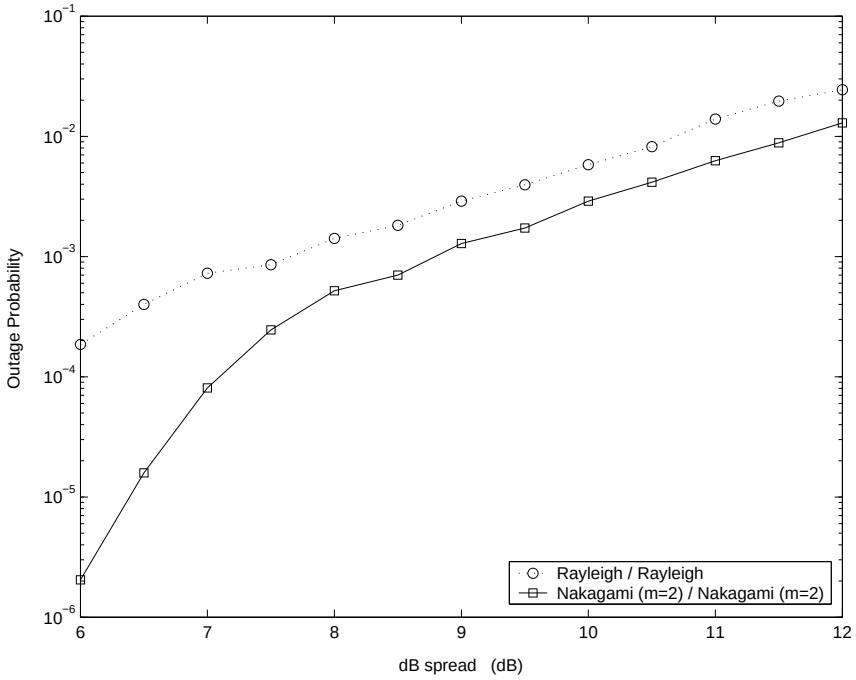

Figure 4.4: Average outage probability versus shadowing factor, where the shadowing factor is identical for all users, which varies from 6 to 12 dB. The desired signal and interferers are all subjected to (i) Rayleigh fading and (ii) Nakagami fading ($m=2$), with each case represented by dotted line and solid line, respectively. $F_{11} = 1$, $F_I = 10^{-5}$.

10^{-3} and $\Upsilon = 10^{-6}$, as illustrated in Fig. 4.5 and Fig. 4.6, respectively, for the case where $F_{11}/F_I = 10^3$ and $F_{11}/F_I = 10^5$. All users have identical shadowing factor and identical fading severity parameter m. Our results show that the average system throughput performance degrades when a lower target BER is imposed. This is because smaller constellation size is more probable of being selected to achieve a lower target BER. However, for a system with larger average SIR as in Fig. 4.6, the above phenomenon is less obvious when the shadowing factor is moderate (6 dB), because the relatively high SIR compensates the negative effect of fading and shadowing. The performance, however, continues to degrade significantly as the shadowing becomes more severe. This result

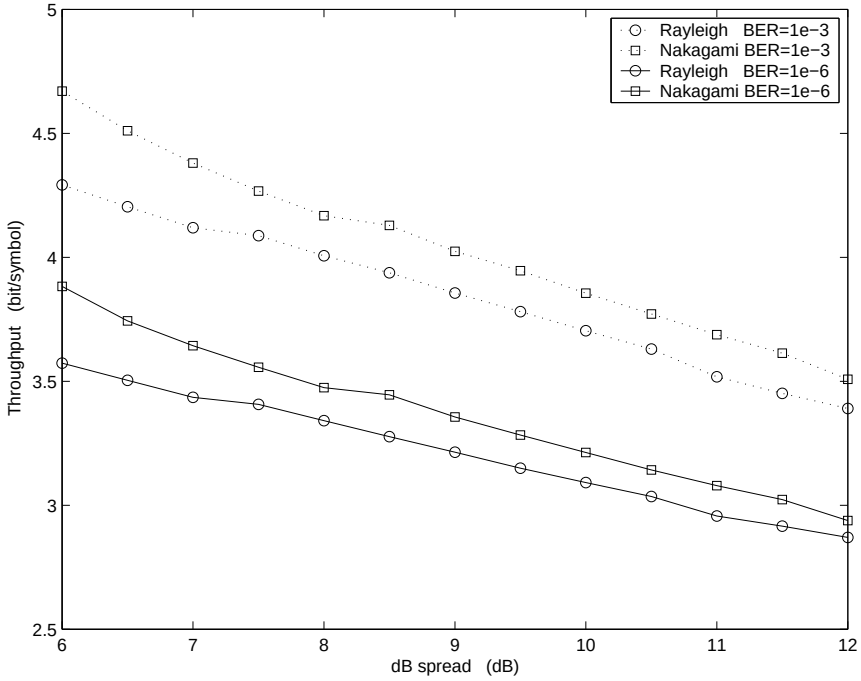

Figure 4.5: Average throughput of MQAM versus shadowing factor for different target BER, $\Upsilon = 10^{-3}$ and $\Upsilon = 10^{-6}$, with each case represented by dotted and solid line, respectively. The shadowing factor is identical for all users, which varies from 6 to 12 dB. All users are subjected to (i) Rayleigh fading and (ii) Nakagami fading ($m = 2$). $F_{11} = 1$, $F_I = 10^{-3}$.

shows that log-normal shadowing can result in worse throughput performance of adaptive MQAM under co-channel interference quite significantly even at large SIR.

4.5 Conclusions

In this chapter, we derive the approximate PDF of the instantaneous received SIR in interference-limited cellular systems under Nakagami fading with shadowing. Average throughput per user and average outage probability per user in such an adaptive MQAM modulation are evaluated and presented. Effects of varying fading and shadowing parameters as well as target BER have been

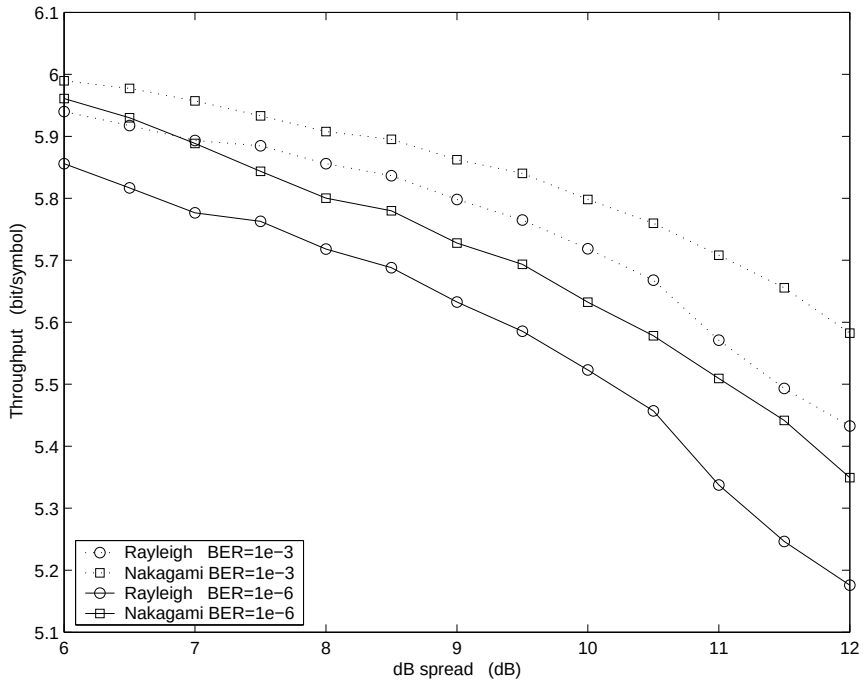

Figure 4.6: Average throughput of MQAM versus shadowing factor for different target BER, $\Upsilon = 10^{-3}$ and $\Upsilon = 10^{-6}$, with each case represented by dotted and solid line, respectively. The shadowing factor is identical for all users, which varies from 6 to 12 dB. All users are subjected to (i) Rayleigh fading and (ii) Nakagami fading ($m = 2$). $F_{11} = 1$, $F_I = 10^{-5}$.

discussed. As expected, the adaptive MQAM achieves higher throughput and and lower outage probability for channels with smaller shadowing factor, but its performance degrades significantly with increasing shadowing factor.

In the next chapter, we will study and derive the transmitter power allocation algorithm for MIMO system.

Chapter 5

Constrained Power Allocation Algorithm for Rate Adaptive MIMO System

Recently, to mitigate fading and its deleterious impact, there is a great interest in applying MIMO technique in wireless communication systems. Multiple antennas implemented at both transmitter and receiver promise significant data throughput, as reported in the pioneer work by Telatar [21] and Foschini [30].

Adaptive modulation is another important technique for increasing data throughput by adapting the modulation size according to the varying channel conditions. It is expected that higher data throughput can be achieved by incorporating adaptive modulation into MIMO system. However, the question is: to maximize the data throughput given a total power constraint, how shall we allocate the power across the antennas?

It has been shown in [21] that the optimal power allocation is given by the water-filling solution, which is obtained by assuming ideal coding and continuous modulation constellation size. However, practical considerations such as discrete constellation sizes, and QoS specification in terms of the required BER performance, are necessary. In [37], the Hughes-Hartog algorithm (H-H) is proposed for multi-carrier systems. The H-H algorithm is optimal for both maximising the data throughput (given total power budget) as well as minimising the total allocated power (given a target total data throughput). However, this algorithm requires quite intensive amount of sorting, and therefore involves significant computation complexity [38]. In [38] [39], alternative low-complexity algorithms have been proposed for the DMT systems. However, in some cases the loss in data throughput is considerable.

The algorithm that has been proposed in [41] is simple, and yet is efficient for high data rate *orthogonal frequency division multiplexing* (OFDM) systems. However, we have observed that this algorithm could lead to considerable loss of data throughput in MIMO systems. This is in contrast to the case of OFDM systems, where the loss is negligible because of high data rate transmission. Recently, the same issue has been addressed in [36] in for wireless MIMO systems. The authors proposed a water-filling based (QoS-WF) algorithm to maximize the total data throughput. However, we note that to achieve the optimal data throughput, the QoS-WF algorithm may cost more power compared to the H-H

algorithm [1].

In this work, we focus on the power allocation problem in QAM modulated MIMO system. We first analyze the optimal power allocation strategy indicated by H-H algorithm and reveal the underlying idea of the optimal power allocation strategy. A new index, so-called *power-increment-to-throughput-improvement ratio* (PITIR), is then introduced, based on which we derive and propose a simple and efficient power allocation algorithm. The proposed algorithm is simpler and easier to implement, while it can achieve almost the same performance as the optimal H-H algorithm [37] in terms of the achieved data throughput and the power efficiency. Moreover, by utilizing the power allocation results obtained in the previous transmissions, the proposed algorithm can avoid some unnecessary computation in the subsequent transmissions, which means the total computation complexity for the whole communication process can be further reduced.

The rest of this chapter is organized as follows. The system model is introduced in Section 5.1. In Section 5.2, we describe the adaptive modulation with discrete constellation sizes in MIMO systems. In Section 5.3, we derive and propose the power allocation algorithm for maximizing the data throughput based on the PITIR. Numerical results and comparison are presented in Section 5.4, and conclusions are drawn in Section 5.5.

[1]Due to discrete number of modulation sizes, the total allocated power may be less than the given power budget in most cases.

5.1 System Model

We consider a MIMO system with N_T transmit antennas and N_R receive antennas. The information data is transmitted simultaneously from all the N_T transmit antennas. We assume that the link gain of each of the $N_T \times N_R$ wireless links is an independent complex Gaussian variable (i.e., we assume independent Rayleigh fading), and the fading process is slow such that it can be approximated as a constant over sufficiently large number of symbols. The received signal is [21]

$$\mathbf{r} = \mathbf{H}\mathbf{s} + \mathbf{n} \tag{5.1}$$

where $\mathbf{s} = [s_1 \cdots s_{N_T}]^T$ and $\mathbf{r} = [r_1 \cdots r_{N_R}]^T$ are, respectively, the $N_T \times 1$ transmitted signal vector and the $N_R \times 1$ received signal vector. The $\mathbf{n} = [n_1 \cdots n_{N_R}]^T$ is an $N_R \times 1$ complex AWGN vector, with independent elements of identical power σ_N^2, $\mathbf{H}$ is the channel coefficients matrix with elements $\{h_{ij}\}$, $1 \leq i \leq N_T$ $1 \leq j \leq N_R$, where h_{ij} represents the complex link gain from transmitter j to receiver i. Note that h_{ij} is a complex Gaussian random variable with zero mean and unit variance.

By the singular value decomposition (SVD) theorem, the channel coefficients matrix $\mathbf{H}$ can be decoupled as

$$\mathbf{H} = \mathbf{W}\mathbf{D}\mathbf{V}^H \tag{5.2}$$

where $\mathbf{D}$ is an $N_R \times N_T$ non-negative and diagonal matrix with diagonal entries

referred to as the singular values of $\mathbf{H}$. The operator $\mathbf{A}^H$ denotes the Hermitian of matrix $\mathbf{A}$. The $\mathbf{W}$ and $\mathbf{V}$ are, respectively, $N_R \times N_R$ and $N_T \times N_T$ unitary matrices. The number of nonzero singular values of $\mathbf{D}$ equals to the rank of $\mathbf{H}$, denoted by l, where $l \leq \min(N_T, N_R)$. Let the l nonzero singular values be denoted by λ_i, $i = 1, 2, \cdots, l$.

By substituting (5.2) into (5.1), we obtained an equivalent channel model consisting of l parallel independent subchannels, known as the eigenchannels [21], with amplitude channel gain λ_i

$$\mathbf{y} = \mathbf{D}\mathbf{x} + \mathbf{n}' \tag{5.3}$$

where $\mathbf{y} = \mathbf{W}^H\mathbf{r}$, $\mathbf{x} = \mathbf{V}^H\mathbf{s}$ and $\mathbf{n}' = \mathbf{W}^H\mathbf{n}$. We order the eigenchannels according its singular value λ_i in a descending manner, i.e., $\lambda_1 \geq \lambda_2 \geq \cdots \geq \lambda_l \geq 0$. Assuming that p_i is the power allocated to the ith eigenchannel, we have $\mathrm{tr}\left(E[\mathbf{x}\mathbf{x}^H]\right) = \sum_{i=1}^{l} p_i$, and

$$\sum_{i=1}^{l} p_i \leq P_T \qquad\qquad p_i \geq 0 \tag{5.4}$$

where P_T is the total power constraint at the transmitter. Thus, the *signal-to-noise ratio* (SNR) in the ith eigenchannel is given by

$$\gamma_i = \frac{\lambda_i^2 p_i}{\sigma_N^2} \qquad\qquad i = 1, \cdots, l \tag{5.5}$$

5.2 Adaptive Modulation in Eigenchannels

Adaptive modulation is applied to each eigenchannel independently through adjusting the constellation size according to the channel quality at the beginning of each transmission. The constellation size is selected from a finite set, denoted by $S=\{S_i\}_0^s$. To meet the BER requirement Υ, τ_i, the BER in the ith eigenchannel, should satisfy

$$\tau_i \leq \Upsilon \tag{5.6}$$

where Υ is the target BER, and we can set $B_i=0$ for those eigenchannels with no transmission. A mapping for τ_i, S_i and γ_i can be found in [85] and can be used to decide the SNR switching threshold, which is the minimum required SNR for a specific constellation size S_i to achieve Υ. Let the SNR threshold set be denoted by $\kappa=\{\kappa_i\}_0^s$, where $\kappa_0=0$ corresponds to no transmission. The modulation selection rule can be simply expressed as: *select* S_i *if* $\kappa_i \leq \gamma < \kappa_{i+1}$, $i < s$; *otherwise select* S_s.

It is well known that there is approximately 3 dB difference between the adjacent thresholds [38] [83], i.e., $\kappa_i = 2^{i-j}\kappa_j$, $i > j > 0$. When the constellation size is changed from S_j to S_i with $i > j \geq 0$, we denote the required increase of

SNR as $\Delta\gamma^{j\to i} = \kappa_i - \kappa_j$. Thus,

$$\begin{cases} \Delta\gamma^{0\to 1} \simeq \Delta\gamma^{1\to 2} \\ \Delta\gamma^{i+1\to i+2} \simeq 2 \cdot \Delta\gamma^{i\to i+1}, \qquad i \geq 1 \end{cases} \tag{5.7}$$

The corresponding power in the kth eigenchannel is obtained by

$$\Delta P_k^{j\to i} = \frac{\Delta\gamma^{j\to i} \cdot \sigma_N^2}{\lambda_k^2} \tag{5.8}$$

Note that in this work, we will use the approximation of (5.7) in deriving the proposed algorithm. In Section 5.4, we shall use simulation to show that the proposed algorithm is effective for practice.

The total data throughput during one transmission is given by

$$T = \sum_{i=1}^{l} T_c^{(i)} \tag{5.9}$$

where $T_c^{(i)} = \log_2 s_i$, is the throughput in the ith eigenchannel. s_i is the constellation size in the ith subchannel.

5.3 Constrained Power Allocation Algorithm

5.3.1 Optimal power allocation rules

Our objective is to optimally distribute the power in order to maximize the data throughput C under the total power constraint (5.4) and BER constraint (5.6). An optimization problem can be thereby formulated as

$$\begin{aligned} \max \quad & T \\ \text{s.t.} \quad & \textstyle\sum_{i=1}^{l} p_i \leq P_T \\ & \tau_i \leq \Upsilon, \qquad i = 1, \cdots, l \\ & S_i = 0, 2, 4, 8, 16, \cdots, s \end{aligned} \tag{5.10}$$

where T is the total data throughput defined in (5.9).

To facilitate our derivation, we define the concepts

- *activate*: action of changing the modulation size from S_0 to S_1,
- *upgrade*: action of changing the modulation size from S_i to S_{i+1} for $0 < i < s$,
- *power-increment-to-throughput-improvement ratio* (PITIR), which is defined as the ratio of the required power increment to the throughput improvement in one action. When an action is to change the constellation size from S_j to S_i in the kth eigenchannel, the corresponding PITIR of this action is given

by

$$\mathrm{PITIR}_k^{j\to i} = \frac{\Delta P_k^{j\to i}}{\log_2 S_i - \log_2 S_j} \tag{5.11}$$

The PITIR is a key performance index used by us to indicate the power efficiency of one action (activating or upgrading). The lower the PITIR, the more power efficient the action, that is, an increment of power can bring a greater improvement of data throughput. Note that this is the same idea behind the H-H algorithm in [37] which always allocates one bit at a time to the subcarrier in multi-carrier requiring the least power system and repeats such a process.

Since the optimal power allocation can be achieved by performing one action at one time, or equivalently adding one bit at one time [37], we have the following important rules which define the optimal strategy for power allocation.

Rule 1: *Always allocate the power first to the eigenchannel which is to perform an action with the lowest PITIR.*

If the PITIR of two actions are equal, we define

Rule 2: *If two actions have identical PITIRs, perform the action in the eigenchannel with higher channel gain.*

Therefore, we need to compare the PITIR for two actions ($i < j$): *A.* $S_a \to S_{a+1}$ in the ith eigenchannel; *B.* $S_b \to S_{b+1}$ in the jth eigenchannel. Substituting (5.8) into (5.11), we have

$$\frac{\mathrm{PITIR}_i^{a\to a+1}}{\mathrm{PITIR}_j^{b\to b+1}} = 2^{a-b} \cdot \frac{\lambda_j^2}{\lambda_i^2} \tag{5.12}$$

If the right-hand side (rhs) of (5.12) is less than or equal to one, A should be performed before B, and vice versa.

In addition, from (5.8) and (5.11), we note that for every eigenchannel, the activating action and the first upgrading action (immediately after the activating) have the same PITIR. Therefore, we shall combine these two actions in our analysis, and treat them as one action (activating) with two bits of throughput improvement, and therefore use $\{S'_i\}_0^{s-1}$ instead of $\{S_i\}_0^s$, where $S'_0 = S_0$ and $S'_i = S_{i+1}$ for $1 \leq i \leq s-1$.

5.3.2 Proposed Power Allocation Algorithm

By taking logarithm based on 2 at the rhs of (5.12), we have $(a-b)+\log_2 \frac{|\lambda_i|^2}{|\lambda_j|^2}$. Suppose $i \geq j$ and $n_{ij}-1 \leq \log_2 \frac{\lambda_i^2}{\lambda_j^2} < n_{ij}$, where n_{ij} is a positive integer. From **Rule 1** and **Rule 2**, we have two facts. Firstly, the ith eigenchannel will be upgraded to modulation size $S'_{b+n_{ij}}$, and secondly, when the action has *just*[2] completed in the ith eigenchannel, the modulation size of the jth eigenchannel is S'_b. Thus, n_{ij} can be viewed as the difference between the modulation modes of the ith and jth eigenchannel due their different PITIR's.

Define $\delta_{i(i+1)} = n_{1(i+1)} - n_{1i}$ for $i > 1$, and $\delta_{12} = n_{12}$. Given $\mathbf{\Lambda} = [\delta_{12}\ \delta_{23}\ \cdots\ \delta_{(l-1)l}]$, we can outline the modulation modes of other eigenchannels at the time when the 1st eigenchannel has just completed one action, as shown in Fig. 5.1a. We shall call it as *line of modulation difference* (LMD), and denote the number of

[2]Here, '*just*' means the moment when an action is completed in the current channel and the next action has not begun.

bits below the LMD by b_{to}.

Furthermore, if we shift the set of LMD up or down, as shown in Fig. 5.1b, we can obtain another set of LMD, $\{\text{LMD}_i\}$, and the corresponding set of b_{to} as $\{b_{to,\,i}\}$, respectively. However, we find that if there are some $\delta_{i(i+1)} > s$, some elements in $\{b_{to,\,i}\}$ are equal. Thus, to differentiate the entries in $\{b_{to,\,i}\}$, we define $\mathbf{\Lambda}' = [\delta'_{12}\ \delta'_{23}\ \cdots\ \delta'_{(l-1)l}]$, where $\delta'_{i(i+1)} = \min\left(s, \delta_{i(i+1)}\right)$, and $\min(x_1, x_2)$ denotes the minimum value of x_1 and x_2. By denoting the number of entries in $\{b_{to,\,i}\}$ as N_b, we have $N_b = s + \sum_{i=1}^{l-1} \delta'_{i(i+1)} + 1$. Note that there is one-by-one relationship between $\{\text{LMD}_i\}$ and $\{b_{to,\,i}\}$. We illustrate of the above results in Fig. 5.1c.

We have $b_{to,\,i} = \sum_{j=1}^{l} t_{i,\,j}$, where $t_{i,\,j} = s_j$ is the number of bits allocated to the jth eigenchannel,

$$t_{i,\,j} = \min\left(O\left(-\sum_{k=1}^{j-1} \delta'_{k(k+1)} + i\right), s\right) \tag{5.13}$$

where the function $O(x)$ is defined as: $O(x) = x$, if $x > 1$; $O(x) = 0$, otherwise. Consequently, the modulation size in the jth eigenchannel is given by $2^{t_{i,\,j}}$. The power allocated to each eigenchannel $p_{i,\,j}$, and the total allocated power $p_{to,\,i} = \sum_{j=1}^{l} p_{i,\,j}$, can then be computed.

To optimally allocate the power given a total power budget (constraint), we first find the index K_o such that $P_T = p_{to,\,K_o}$ or $p_{to,\,K_o} < P_T < p_{to,\,K_o+1}$. If $P_T = p_{to,\,K_o}$, the optimal solution can then be obtained from (5.13). Some

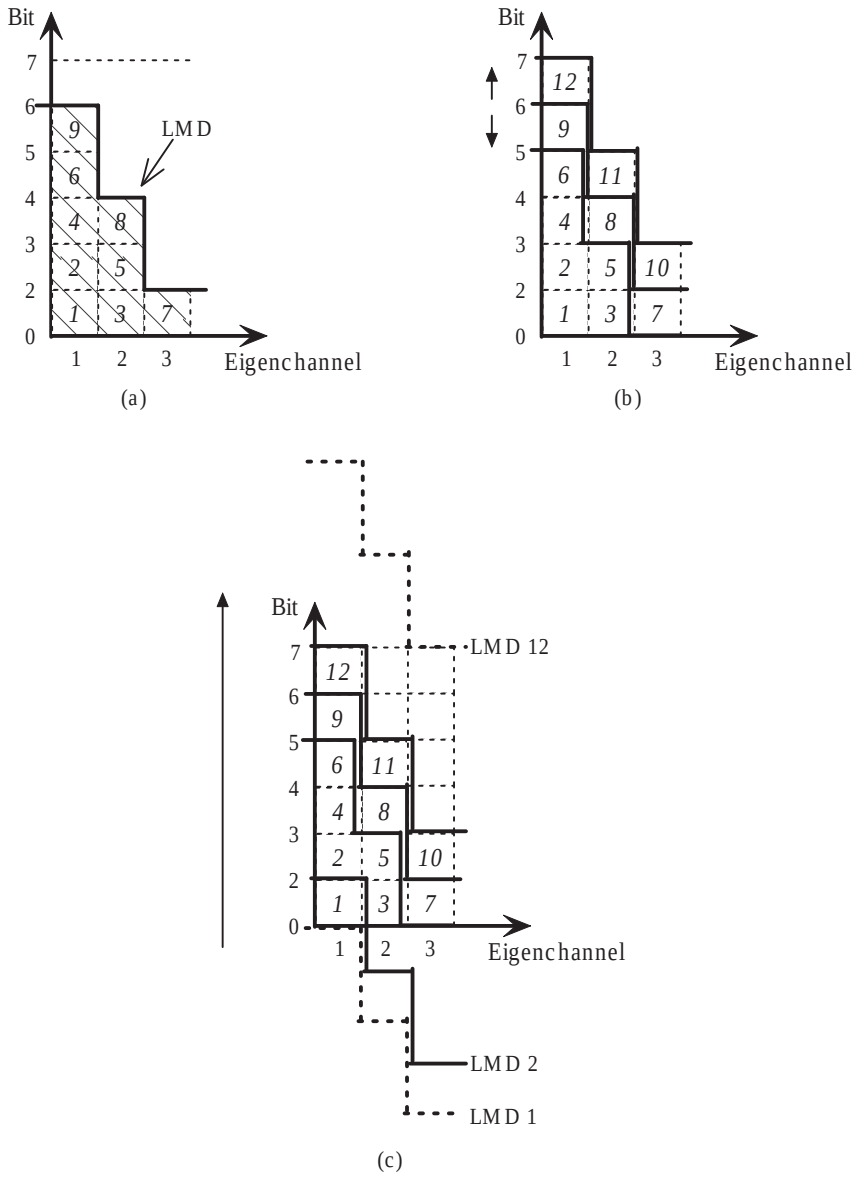

Figure 5.1: A MIMO system with 3 eigenchannels, where the maximal modulation size $m = 7$ and $\mathbf{\Lambda}' = [2\ 2]$. Each square corresponds to one action. $N_b = 12$. The italic number in each square is the order index of the action in optimal power allocation following **Rule 1** and **Rule 2**.

search method such as the bisection search in [86] can be used for this purpose. If $P_T = p_{to,i}$, the optimal solution can be obtained from (5.13). If $p_{to,K_o} < P_T < p_{to,K_o+1}$, we can redistribute the residual power to eigenchannels based on the solution corresponding to p_{to,K_o}. Since $1 < b_{to,i+1} - b_{to,i} < l$ when $i > 0$, such adjustment is relatively simple.

The proposed algorithm can be summarized as:

Step 1 : Combine the activating action and the immediate next upgrading action in each eigenchannel as a single activating action. Compute $\mathbf{\Lambda}'$.

Step 2 : Find p_{to,K_o} such that $p_{to,K_o} \leq P_T < p_{to,K_o+1}$ or $(p_{to,K_o} = P_T)$ by using the bisection method [86] (or any other efficient search method): Use search method to select an index i in each iteration, compute $b_{to,i}$ and the corresponding $p_{to,i}$. Then, compare $p_{to,i}$ with P_T, and decide the direction of selecting next i (see details in [86]).

i. If $P_T = p_{to,K_o}$, then $T = b_{to,K_o}$ and the corresponding power allocation solution is given by $p_{K_o,j}$, for $j = 1, \cdots, l$.

ii. If $p_{to,K_o} \leq P_T < p_{to,K_o+1}$, go to **Step 3**.

Step 3 : Compute the residual power $p_r = P_T - p_{to,K_o}$. For $j = 1 : l$, compute the PITIR of the action in the jth eigenchannel which is to be performed next. Then, if p_r can support, perform the actions (less than l) from the one with the lowest PITIR to the one with the highest PITIR. Note that if the action to be performed is to activate the eigenchannel, detach the action to two separated ones (one activating and one upgrading, as we have combined two bits at the

beginning), and perform them consecutively.

5.3.3 Discussion on complexity of the proposed algorithm

In **Step 2**, to search for p_{to,K_o} in $\{p_{to,i}\}$ by using bisection method, we need (at most) approximately $\log_2(N_b)$ iterations, where $N_b = s+\sum_{i=1}^{l-1}\delta'_{i(i+1)}+1$ and therefore $N_b \leq sl$. The power adjustment in **Step 3** requires only one sorting of $(l-1)$ PITIR values. Based on this argument, the resulting complexity of the proposed algorithm is less than the complexity of **Step 2** or **Step 3**. Therefore, it is simpler than the H-H algorithm in [37], which requires N_b iterations and one sorting of l variables in each iteration.

On the other hand, in wireless MIMO channels, $\mathbf{H}$ (and therefore λ_i) can vary randomly from data block to data block due to fading. The power allocation algorithm should therefore be able to track this change and update the power allocation accordingly. Most previously published schemes in [36, 37, 40] focus on how to reduce the complexity of power allocation within a transmission. Here, we focus how to make use of the results obtained in earlier transmission to reduce the computation in subsequent transmissions.

In the proposed algorithm, $\{b_{to,i}\}$ and $\{t_{i,j}\}$ only depend on $\mathbf{\Lambda}'$, the entries of which can only be the integers between 0 and s, as shown in Section 5.3.2. This means that the proposed algorithm virtually shrink the range of time-varying parameters. In the next section, we show that although the channel

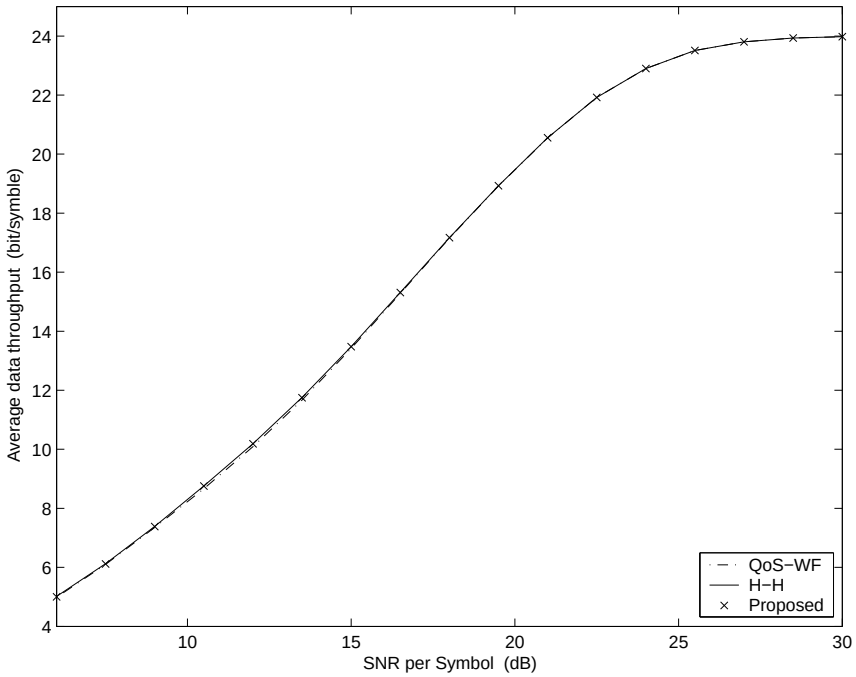

Figure 5.2: Comparison of average data throughput between the proposed algorithm, H-H algorithm in [24] and QoS-WF algorithm in [28] for a MIMO system with 6 transmit and 4 receive antennas. $B_t = 10^{-3}$.

gain of eigenchannel is varying due to fading, it is still highly probable that a fix $\mathbf{\Lambda}'$ can be observed throughout data transmission. Since a fixed $\mathbf{\Lambda}'$ results in the fixed $\{b_{to,i}\}$ and $\{t_{i,j}\}$, we can therefore store $\mathbf{\Lambda}'$, $\{b_{to,i}\}$ and $\{t_{i,j}\}$ in lookup tables. This can reduce the computational load during transmission, because the transmitter can now simply refer to the lookup table for a same $\mathbf{\Lambda}'$ in subsequent transmissions. This makes the proposed algorithm a more attractive candidate for wireless MIMO systems.

5.4 Numerical Results

In this section, we compare the proposed algorithm with the H-H algorithm in [37] and QoS-WF algorithm in [36]. We assume the channel is subject to

flat fading. Each entry of the channel matrix $\mathbf{H}$ is a complex Gaussian random variable with zero mean and unit variance. Without loss of generality, the total power budget is normalized to one, and as a result, the SNR per symbol given by $1/\sigma_N^2$. The MQAM is adopted in each eigenchannel, where $\{S_i = 2^i\}$, $i = 1, \cdots, 6$. The target BER is set to 10^{-3}. Note that even though we have used the approximation in (5.7) to derive the algorithm, the accurate SNR threshold values computed in [66] is used in our simulation to verify how effective is the proposed algorithm in practice.

We vary the SNR from 6 to 30 dB with 1.5 dB interval, and at each SNR value, we generate $100,000$ channel realizations to acquire sufficient statistics of the fading channel. In Fig. 5.2 we compare the average data throughput of these three algorithms, each is obtained by averaging the total data throughput over different channel realizations. We see that these three algorithms almost achieve the same data throughput over wide range of SNR values. Therefore, the use of approximated SNR thresholds in our derivation has negligible effect on the performance of the proposed algorithm.

We note that for the same data throughput, different bit allocation in different eigenchannels will result in different total allocated power. We therefore calculate the total allocated power by averaging over all the channel realizations for various SNR. As shown in Fig. 5.3, the total allocated power of our proposed algorithm is very close to those of the H-H algorithm in the whole range of SNR. However, at lower SNR region, the QoS-WF algorithm utilizes

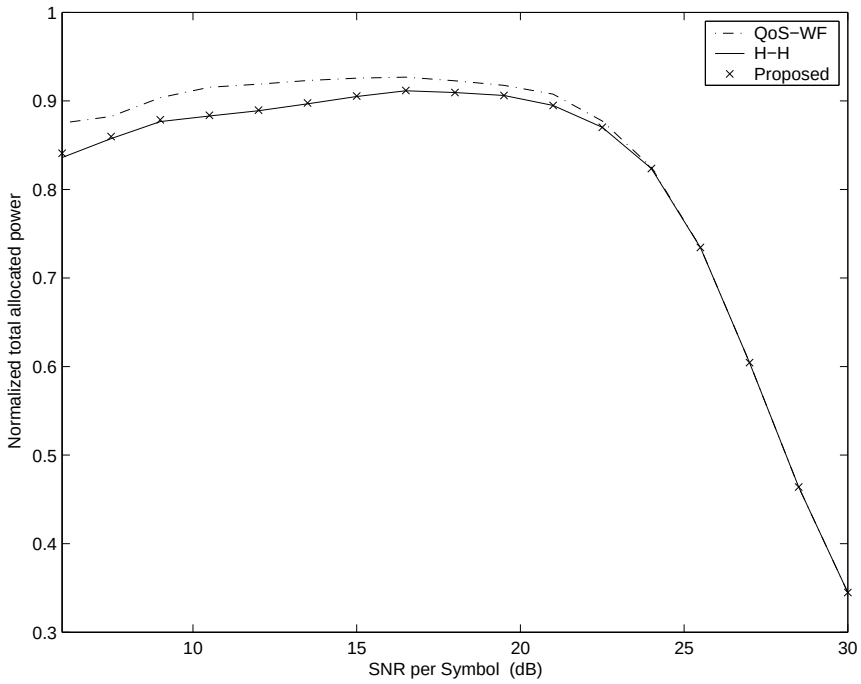

Figure 5.3: Comparison of total allocated power between the proposed algorithm, H-H algorithm in [24] and QoS-WFalgorithm in [28] for a MIMO system with 6 transmit and 4 receive antennas. $B_t = 10^{-3}$.

more power than the other two schemes. The difference between the total allocated power of these three schemes decreases as SNR increases, and these three curves match for SNR > 25 dB. This is because as SNR increases, all eigenchannels tend to use the maximum modulation size. Therefore, the power allocated to each eigenchannel tends to be fixed, which results in the same modulation size and same power allocation in each eigenchannel.

We also randomly generate 10^6 MIMO channel realizations for the system described above, and then compute the corresponding $\mathbf{\Lambda}'$ for each realization. From our result, we find that only 91 $\mathbf{\Lambda}'$ with at least one different entry are found. Therefore it is highly probable that the same $\{b_{to,i}\}$ and $\{t_{i,j}\}$ occur throughout the transmission of a long stream of many symbols or blocks).

Thus, we conclude that by using the proposed algorithm, a large amount of computation can be avoided if some previous results are stored in tables.

5.5 Conclusions

In this chapter, we propose a simple and yet efficient power allocation algorithm for MIMO systems adopting adaptive modulation with discrete QAM modulation sizes. Numerical results and comparison have been presented and discussed. The proposed algorithm achieves almost the same throughput performance and total power consumption as a previously published scheme in [37].

Chapter 6

Conclusions and Future works

In fading channels, transmitted power control can play a significant role to combat co-channel interference, and adaptive modulation is an efficient way to utilize the radio spectrum. Both techniques play its important role for high data rate wireless transmission in future communication systems.

6.1 Conclusions

This thesis begins with the study in the minimization of outage probabilities for users in an interference-limited system subject to Nakagami fading. We have highlighted and described the inherent relationship between the newly proposed performance index, SIRM, the outage probability requirement, and the fading parameters of desired signal and interferers in Nakagami channels. We then derived and studied a new optimal power control scheme for interference-limited Nakagami channels, with the objective of balancing outage probability for a system of mobile users.

We further show that it is feasible to maximize the SIRM to approximately achieve the objective of balancing outage probability, and this problem can be easily solved by using the Perron-Frobenius theory. We also find that in spite of the rapid variation of Nakagami fading, the transmitter power can be updated in the time scale of large scale fading, such as log-normal shadowing, to achieve outage probability balancing.

In addition, we have developed a framework to analyze the throughput performance of adaptive modulation in the presence of log-normal shadowing, Nakagami fading and co-channel interference. We derive the approximate expression of PDF for the instantaneous received SIR in interference-limited cellular systems, subjected to Nakagami fading and shadowing. Consequently, the average system throughput and outage probability performance of adaptive MQAM modulation under co-channel interference have been evaluated and presented in this work. The effects of varying fading and shadowing parameters as well as the target BER have been studied and discussed. As expected, the adaptive MQAM achieves higher throughput and and lower outage probability for channels with smaller shadowing spread, but its performance degrades significantly with increasing shadowing spread.

Lastly, we investigate the power allocation problem in MIMO systems adopting adaptive MQAM modulation of discrete constellation sizes. Based on the idea of optimal bit allocation in multicarrier system [37], we propose a new index, so-called *power-increment-to-throughput-improvement ratio* (PITIR), to

derive and propose a simple and efficient power allocation algorithm for MIMO systems. The proposed algorithm achieves almost the same throughput performance as the previous optimal algorithm in [37]. It also achieves a better power efficiency in power allocation than the algorithm in [36] which has been also proposed for rate adaptive MIMO systems with discrete modulation sizes. Though it is not shown in this thesis, the proposed algorithm can be modified and applied to the power and bit allocation problem in multicarrier system. We also highlight that the approximation of the SIR threshold in adaptive MQAM modulation does not affect the performance of the proposed algorithm. From this viewpoint, careful consideration of the channel condition and the practical modulation modes is necessary to solve the power allocation problem.

6.2 Future Works

For the proposed algorithm in Chapter 3, two major directions for future works can be considered. Firstly, we can further consider the maximum transmitter power constraint in real systems. In such a case, the power solution directly obtained from (3.22) may violate the constraint, i.e., one or more transmitter power is larger than the constraint. Obviously, this will make the optimization problem more complicated. Sometimes, users who need a very large transmitter power may have to be removed from the system to allow other users to have an acceptable transmission quality. Secondly, the outage probability in Chapter 3 is computed within only one power control cycle (that is, the time

scale of long term fading), i.e., it does not take into account the statistics of the log-normal shadowing. Thus, it is still unclear how the outage probability will be affected by the lognormal statistics if the proposed algorithm is to be used.

Another interesting direction is to jointly consider power control and adaptive modulation for multiuser system in fading channels. For future wireless communication system, multiple type of services with different rate and different QoS requirements are to be supported. It is therefore worthy of looking into how to meet the service requirement for different users by using power control and adaptive modulation. From system design viewpoint, we could optimize the system for high data rate and large capacity, while maintaining appropriate fairness of service for multiple users.

The channel model in Chapter 5 is simple flat fading. In future works, complex channel models which include correlation, multipath and etc. could all be taken into consideration. Furthermore, combination of power allocation with other techniques such as antenna selection would be a promising direction. In addition, since space-time coding is a strong candidate for MIMO system, coding scheme could also be investigated jointly with the optimal power allocation strategy.

References

[1] F. Bock and B. Ebstein, "Assignment of transmitter powers by linear programming," *IEEE Transactions on Electromagnetic Compatibility*, vol. 6, no. 2, pp. 36–44, 1964.

[2] J. M. Aein, "Power balancing in systems employing frequency reuse," *COMSAT Technical Review*, vol. 3, no. 2, pp. 277–300, 1973.

[3] H. Alavi and R. W. Nettleton, "Downstream power control for a spread spectrum cellular mobile radio system," in *Proc. IEEE GLOBECOM'82*, 1982, pp. 84–88.

[4] R. W. Nettleton and H. Alavi, "Power control for a spread spectrum cellular mobile radio system," in *Proc. IEEE VTC*, 1983, pp. 242–246.

[5] J. Zander, "Performance of optimum transmitter power control in cellular radio systems," *IEEE Trans. Veh. Technol.*, vol. 41, pp. 57–62, Feb. 1992.

[6] S. A. Grandhi, R. Vijayan, D. J. Goodman, and J. Zander, "Centralized power control in cellular systems," *IEEE Trans. Veh. Technol.*, vol. 42, no. 4, pp. 466–468, 1993.

[7] J. Zander, "Transmitter power control for co-channel interference management in cellular radio systems," in *Proc. 4th WINLAB Workshop on Third Generation Wireless Information Networks*, 1993, pp. 241–147.

[8] A. Sudheer, V. Rajiv, and G. David, "Centralized power control in cellular radio systems," *IEEE Trans. Veh. Technol.*, vol. 42, pp. 466–468, Nov. 1993.

[9] J. Zander, "Distributed co-channel interference control in cellular radio systems," *IEEE Trans. Veh. Technol.*, vol. 41, no. 3, pp. 305–311, 1992.

[10] S. A. Grandhi, R. Vijayan, D. J. Goodman, and J. Zander, "Distributed power control in cellular radio systems," *IEEE Trans. Veh. Technol.*, vol. 42, no. 2/3/4, pp. 226–228, 1993.

[11] G. J. Foschini and Z. Miljanic, "A simple distributed autonomous power control algorithm and its convergence," *IEEE Trans. Veh. Technol.*, vol. 42, no. 4, pp. 641–646, 1993.

[12] D. Mitra, "An asynchronous distributed algorithm for power control in cellular radio systems," in *Proc. 4th WINLAB Workshop*, 1993, pp. 249–259.

[13] S. A. Grandhi, J. Zander, and R. Yates, "Constrained power control," *Wireless Personal Communications*, vol. 1, no. 4, pp. 257–270, 1995.

[14] R. Jäntti and S.-L. Kim, "Second-order power control with asymptotically fast convergence," *IEEE J. Select. Areas Commun.*, vol. 18, no. 3, pp. 447–457, 2000.

[15] ——, "Power control with partially known link gain matrix," in *Proc. IEEE ICC*, vol. 2, 2002, pp. 882–886.

[16] M. Almgren, H. andersson, and K. Wallstedt, "Power control in cellular system," in *Proc. IEEE VTC*, vol. 2, 1994, pp. 833–837.

[17] R. D. Yates, S. Gupta, C. Rose, and S. Sohn, "Soft dropping power control," in *Proc. IEEE VTC*, vol. 3, 1997, pp. 1694–1698.

[18] T.-H. Lee, J.-C. Lin, and Y. T. Su, "Downlink power control algorithms for cellular radio systems," *IEEE Trans. Veh. Technol.*, vol. 44, no. 1, pp. 89–94, 1995.

[19] M. Andersin, Z. Rosberg, and J. Znder, "Gradual removals in cellular pcs with constrained power control and noise," *IEEE/ACM Wireless Networks Journal*, vol. 2, no. 1, pp. 27–43, 1996.

[20] L. H. Brandenburg and A. D. Wyner, "Capacity of the gaussian channel with memory: The multivariate case," *Bell Syst. Tech. J.*, vol. 53, no. 5, pp. 745–778, 1974.

[21] I. E. Telatar, "Capacity of multi-antenna gaussian channels," *European Transactions on Telecommunications*, vol. 10, pp. 585–595, Nov./Dec. 1999.

[22] N. Al-Dhahir and J. M. Cioffi, "Block transmission over dispersive channels: Transmit filter optimization and realization and MMSE-DFE receiver performance," *IEEE Trans. Inform. Theory*, vol. 42, pp. 137–160, Jan. 1996.

[23] G. G. Raleigh and J. M. Cioffi, "Spatio-temporal coding for wireless communication," *IEEE Trans. Commun.*, vol. 46, pp. 357–366, Mar. 1998.

[24] A. Scaglione, S. Barbarossa, and G. B. Giannakis, "Filterbank transceivers optimizing information rate in block transmissions over dispersive channels," *IEEE Trans. Inform. Theory*, vol. 45, pp. 1019–1032, Apr. 1999.

[25] D. Shiu and J. M. Kahn, "Power allocation strategies for wireless systems with multiple transmit antennas," internal report of the University of California, Berkley and Lucent Technologies, July 1998.

[26] G. Scutari and S. Barbarossa, "Generalized water-filling for multiple transmit antenna systems," in *Proc. ICC*, 2003, pp. 2668 – 2672.

[27] N. Jindal, S. Jafar, S. Vishwanath, and A. Goldsmith, "Sum power iterative water-filling for multi-antenna gaussian broadcast channels," in *the 36th Asilomar Conference on Signals, Systems and Computers*, 2002, pp. 1518 – 1522.

[28] D. J. Mazzarese and W. A. Krzymien, "Throughput maximization and optimal number of active users on the two transmit antenna downlink of a cellular system," in *Proc. PACRIM*, 2003, pp. 28–30.

[29] P. Almers, F. Tufvesson, O. Edfors, and A. F. Molisch, "Measured capacity gain using water filling in frequency selective mimo channels," in *Proc. IEEE PIMRC'02*, 2002, pp. 1347 – 1351.

[30] G. J. Foschini and M. J. Gans, "On limits of wireless communications in a fading environment when using multiple antennas," *Wireless Personal Communications*, vol. 6, pp. 311–335, 1998.

[31] W. Rhee and J. M. Cioffi, "Ergodic capacity of multi-antenna gaussian multiple access channels," in *the 35th Asilomar Conference on Signals, Systems and Computers*, 2001.

[32] L. Zheng and D. N. C. Tse, "Communication on the grassmann manifold: A geometric approach to the noncoherent multiple-antenna channel," *IEEE Trans. Inform. Theory*, vol. 48, pp. 359–383, Feb. 2002.

[33] E. Visotsky and U. Madhow, "Space-time transmit precoding with imperfect feedback," *IEEE Trans. Inform. Theory*, vol. 47, pp. 2632–2639, Sept. 2001.

[34] S. A. Jafar, S. vishwanath, and A. Goldsmith, "Channel capacity and beamforming for multiple transmit and receive antennas with covariance feedback," in *Proc. IEEE ICC*, June 2001, pp. 2266–2270.

[35] S. Bhashyam, A. Sabharwal, and B. Aazhang, "Feedback gain in multiple antenna systems," *IEEE Trans. Commun.*, vol. 50, pp. 785–798, May 2002.

[36] X. Zhang and B. Ottersten, "Power allocation and bit loading for spatial multiplexing in MIMO systems," in *Proc. ICASSP'03*, 2003, pp. 53–56.

[37] D. Hughes-Hartogs, "Ensemble modem structure for imperfect transmission media," U.S. Patent 4 679 227 (July 1987), 4 713 816 (March 1988), 4 833 796 (May 1989).

[38] P. S. Chow, "Bandwidth optimized digital transmission techniques for spectrally shaped channels with impulsive noise," Ph.D. dissertation, Stanford Univ., Stanford, CA, 1993.

[39] P. S. Chow, J. M. Cioffi, and J. A. C. Bingham, "A practical discrete multitone transceiver loading algorithm for data transmission over spectrally shaped channels," *IEEE Trans. Commun.*, vol. 43, no. 3, pp. 773–775, Feb.-Mar.-Apr. 1995.

[40] B. S. Krongold, K. Ramchandran, and D. L. Jones, "Computationally efficient optimal power allocation algorithms for multicarrier communication systems," *IEEE Trans. Commun.*, vol. 48, no. 1, pp. 23–27, Jan. 2000.

[41] J. Jang, K. B. Lee, and Y.-H. Lee, "Transmit power and bit allocations for OFDM systems in a fading channel," in *Proc. GLOBECOM'03*, 2003, pp. 858–862.

[42] P. A. Bello and W. M. Cowan, "Theoretical study of on/off transmission over Gaussian multiplicative circuits," in *Proc. IRE 8th Nat. Communications Symp.*, Utica, N.Y., Oct. 1962.

[43] J. K. Cavers, "Variable rate transmission for Rayleigh fading channels," *IEEE Trans. Commun. Technol.*, vol. COM-20, pp. 15–20, Feb. 1972.

[44] W. T. Webb and R. Steele, "Variable rate qam for mobile radio," *IEEE Trans. Commun.*, vol. 43, no. 7, pp. 2223–2230, 1995.

[45] R. Steele and W. T. Webb, "Variable rate QAM for data transmission over Rayleigh fading channels," in *Proc. Wireless'91*, vol. 43, Calgary, AB, Canada, 1991, pp. 1–14.

[46] M. L. Moher and J. H. Lodge, "TCMP-A modulation and coding strategy for rician fading channels," *IEEE J. Select. Areas Commun.*, vol. 7, pp. 1347–1355, Dec. 1989.

[47] J. K. Cavers, "An analysis of pilot symbol assisted modulation for rayleigh fading channels," *IEEE Trans. Veh. Technol.*, vol. 40, pp. 686–693, Nov. 1991.

[48] S. Sampei and T. Sunaga, "Rayleigh fading compensation for QAM in land mobile radio communications," *IEEE Trans. Veh. Technol.*, vol. 42, pp. 137–147, May 1993.

[49] S. Sampei, S. Komaki, and N. Morinaga, "Adaptive modulation/TDMA scheme for large capacity personal multimedia communicaations systems," *IEICE Trans. Commun.*, vol. E77-B, pp. 1096–1103, Sept. 1994.

[50] L. Hanzo, W. T. Webb, and T. Keller, *Single- and Multi- Carrier Quadrature Amplitude Modulation.* John Wiley, IEEE Press, 2000.

[51] S. Otsuki, S. Sampei, and N. Morinaga, "Square QAM adaptive modulation/TDMA/TDD systems using modulation level estimation with Walsh function," *Electron. Lett.*, vol. 31, pp. 169–171, Feb. 1995.

[52] A. J. Goldsmith and S. g. Chua, "Variable-rate variable-power MQAM for fading channels," *IEEE Trans. Commun.*, vol. 45, pp. 1218–1230, Oct. 1997.

[53] J. M. Torrance and L. Hanzo, "Optimization of switching levels for adaptive modulation in a slow Rayleigh fading channel," *Electron. Lett.*, vol. 32, pp. 1167–1169, 1996.

[54] B. J. Choi, M. Münster, L. L. Yang, and L. Hanzo, "Performance of Rake receiver assisted adaptive-modulation based CDMA over frequency selective slow Rayleigh fading channel," *Electron. Lett.*, vol. 37, pp. 247–249, 2001.

[55] B. Choi and L. Hanzo, "Optimum mode-switching-assisted constant-power single- and multicarrier adaptive modulation," *IEEE Trans. Veh. Technol.*, vol. 52, no. 3, pp. 536–560, May 2003.

[56] W. H. Press, S. A. Teukolsky, W. T. Vetterling, and B. P. Flannery, *Numerical Recipies in C.* Cambridge, U.K.: Cambridge Univ. Press, 1992.

[57] J. Paris, M. del Carmen Aguayo-Torres, and J. Entrambasaguas, "Optimum discrete-power adaptive QAM scheme for Rayleigh fading channels," *IEEE Commun. Lett.*, vol. 5, pp. 281–283, July 2001.

[58] S. T. Chung and A. Goldsmith, "Degrees of freedom in adaptive modulation: A unified view," *IEEE Trans. Commun.*, vol. 49, pp. 1561–1571, Sept. 2001.

[59] X. Qiu and K. Chawla, "On the performance of adaptive modulation in cellular systems," *IEEE Trans. Commun.*, vol. 47, no. 6, pp. 884–895, 1999.

[60] M. S. Alouini and A. J. Goldsmith, "Adaptive modulation over Nakagami fading channels," *Kluwer Journal on Wireless Communications*, vol. 13, no. 1-2, pp. 119–143, May 2000.

[61] T. Eyceoz, S. Hu, and A. Duel-Hallen, "Deterministic channel modeling and long-range prediction of fast-fading mobile radio channels," *IEEE Commun. Lett.*, vol. 2, pp. 254–256, Sept. 1998.

[62] A. Duel-Hallen, S. Hu, and H. Hallen, "Long-range prediction of fading signals: Enabling adaptive transmission for mobile radio channels," *IEEE Signal Processing Mag.*, vol. 17, pp. 62–75, May 2000.

[63] T.-S. Yang, A. Duel-Hallen, and H. Hallen, "Reliable adaptive modulation aided by observations of another fading channel," *IEEE Trans. Commun.*, vol. 52, no. 4, pp. 605–611, Apr. 2004.

[64] S. Falahati, A. Svensson, M. Sternad, and H. Mei, "Adaptive modulation systems for predicted wireless channels," *IEEE Trans. Commun.*, vol. 52, no. 2, pp. 307–316, Feb. 2004.

[65] C. C. Chai, X. Chen, and Y. H. Chew, "Power control for minimum outage in interference-limited Nakagami fading wireless channels," in *Proc. VTC'03 Fall*, 2003, pp. 1549–1553.

[66] X. Chen, C. C. Chai, and Y. H. Chew, "Performance of adaptive MQAM in cellular system with Nakagami fading and log-normal shadowing," in *Proc. IEEE PIMRC'03*, vol. 2, 2003, pp. 1274–1278.

[67] ——, "Constrained power allocation algorithm for rate adaptive mimo system," accepted by IEEE ISSSTA'04, 2004.

[68] S. Kandukuri and S. Boyd, "Optimal power control in interference-limited fading wireless channels with outage-probability specifications," *IEEE Trans. Wireless Commun.*, vol. 1, no. 1, pp. 46–55, Jan. 2002.

[69] S. Schwartz and Y. S. Yeh, "On the distribution function and moments of power sums with log-normal components," *Bell System Tech. J.*, vol. 61, pp. 1441–1462, Sept. 1982.

[70] G. L. Stüber, *Principles of Mobile Communication*, 2nd ed. Boston: Kluwer Academic, 2001.

[71] V. H. M. Donald, "The cellular concept," *The Bell Technical Journal*, vol. 58, no. 1, pp. 15–41, 1979.

[72] J. P. Kermoal, L. Schumacher, K. I. Pedersen, P. E. Mogensen, and F. Fredriksen, "A stochastic MIMO radio channel model with experimental validation," *IEEE J. Select. Areas Commun.*, vol. 20, no. 6, Aug. 2002.

[73] D. Gesbert, H. Bölcskei, D. Gore, and A. Paulraj, "Outdoor MIMO wireless channels: models and performance prediction," *IEEE Trans. Commun.*, vol. 50, no. 12, 2001.

[74] T. S. Rappaport, *Wireless Communications Principles and Practice*. New York: Prentice-Hall, 1996.

[75] M. Nakagami, "The m-distribution – a general formula of intensity distribution of rapid fading," *Statistical Methods in Radio Wave Propagation*, pp. 3–36, 1960.

[76] M. Abramowitz and I. Stegun, *Handbook of Mathematics Functions*. Washington, DC.: National Bureau of Standards, 1972.

[77] A. A. Abu-Dayya and N. C. Beaulieu, "Outage probabilities of cellular mobile radio systems with multiple Nakagami interferers," *IEEE Trans. Veh. Technol.*, vol. 40, pp. 757–768, Nov. 1991.

[78] K. O. Bowman and L. R. Shenton, *Properties of Estimators for The Gamma Distribution*. New York: Marcel Dekker, 1988.

[79] I. S. Gradshteyn and I. M. Ryzhik, *Table of Integrals, Series, and Products*. New York: Academic Press, 1980.

[80] Q. T. Zhang, "Outage probability of cellular mobile radio in the presence of multiple Nakagami interferers with arbitrary fading parameters," *IEEE Trans. Veh. Technol.*, vol. 44, pp. 661–667, Aug. 1995.

[81] A. Annamalai, C. Tellambura, and V. K. Bhargava, "Simple and accurate methods for outage analysis in cellular mobile radio systems — a unified approach," *IEEE Trans. Commun.*, vol. 49, pp. 303–316, Feb. 2001.

[82] J. Papandriopoulos, J. Evans, and S. Dey, "Outage-based optimal power control for generalized multiuser fading channels," *IEEE Trans. Commun.*, submitted for publication.

[83] L. Hanzo, C. H. Wong, and M. S. Yee, *Adaptive Wireless Transceivers: Turbo-Coded, Turbo-Equalized and Space-Time Coded TDMA, CDMA and OFDM Systems*. West Sussex: Wiley, 2002.

[84] P. Cardieri and T. S. Rappaport, "Statistics of the sum of lognormal variables in wireless communications," in *Proc. VTC'00*, 2000.

[85] J. G. Proakis, *Digital Communicaions*, 4th ed. McGraw-Hill, 2001.

[86] C. A. Shaffer, *A Practical Introduction to Data Structures and Algorithm Analysis*, 3rd ed. NJ: Prentice Hall, 2001.